PREPARATION AND CHARACTERIZATION OF EVA-SISAL FIBRE COMPOSITES

by

MAMOOKHO ELIZABETH MALUNKA (B.Sc. Honours)

submitted in accordance with the requirements for the degree

MASTER OF SCIENCE (M.Sc.)

in the

Department of Chemistry
Faculty of Natural and Agricultural Sciences

at the

UNIVERSITY OF THE FREE STATE (QWAQWA CAMPUS)

SUPERVISOR: PROFESSOR AS LUYT

JANUARY 2005

DECLARATION

I, the undersigned, hereby declare that the research in this thesis is my own original work, which has not partly or in full been submitted to any other University in order to obtain a degree.

Mamookho Elizabeth Malunka

DEDICATION

I would like to dedicate this book to my late parents (Halieo P Malunka and Nkupi P Malunka).

ABSTRACT

The main focus of this research project was on sisal fibre as organic filler and the effect of its content on the thermal and mechanical properties of EVA. Sisal is a promising reinforcement for use in composites on account of its low cost, low density, high specific strength and modulus, no health risk, easy availability in some countries and renewability. Ethylene vinyl acetate (EVA) copolymer has a broad range of industrial applications. Uncross-linked and cross-linked EVA and EVA-sisal composites were prepared and characterized. In this work we present and discuss the preparation and characterization of EVA-sisal fibre composites. All the results strongly point to grafting between EVA and sisal, even for samples prepared in the absence of DCP. Gel content results indicate increased cross-linking/grafting with increasing DCP and sisal contents. Grafting between EVA and sisal fibre is confirmed by the porosity and FTIR results. The SEM photomicrographs also support strong fibre-matrix adhesion in the EVA-sisal composites. Grafting, and to a lesser extent cross-linking of EVA, had an impact on the thermal and tensile properties of the composites, because cross-linking and grafting substantially influence the structure and morphology of the composites. The incorporation of sisal in the EVA matrix increases the composites' stiffness. The influence of DCP on the stiffness, however, depends on the amount of sisal in the composite. Elongation at break increases in the presence of DCP, but drastically decreases in the presence of sisal. For pure EVA, stress at break decreases with increasing DCP content, probably because of degradation. It also decreases when 10 % sisal is present in the EVA matrix, but increases for higher sisal contents. In the presence of sisal, increasing DCP content also increases stress at break. Cross-linking and grafting also had an impact on the surface free energy of the samples.

TABLE OF CONTENTS

CHAPTER 1

INTRODUCTION

In our everyday life timber plays a significant role. Timber resources are, however, getting depleted continuously while the demand for the material is ever increasing. According to literature, by the beginning of the next century, wood will be scarce for the whole world [1]. This situation has led to the development of alternative materials. Among the various synthetic materials that have been explored and advocated, plastics claim a major share as wood substitutes. Plastics are used for almost everything from the articles of daily use to the components of complicated engineering structures and heavy industrial applications [2]. Most of them are extensively applied in buildings as flooring materials, because they are resistant to abrasion and have low heat conductivity and water absorption, as well as sufficient hardness and strength. Most of them also fail to swell when moistened, and readily take on varnishes and paints. Hardware items like door and window frames, flushing cisterns, overhead water storage tanks and water fittings are commercially available and are finding acceptance in the building industry [3].

1.1 Composite materials

A composite material is defined as one that uses two or more different types of materials to form a single structure. It has properties that are a combination of the properties of its components. The mixing of the different phases is usually not on the atomic level. The first distinction that can be made is between natural and artificial composite materials. Examples of natural composites are the human bone structure and trees. Bones are not uniform across their area. Their different regions have different properties, and can be modeled using composite mechanics equations [4]. Trees have very oriented mechanical properties, and are also not uniform across their area. However, it is expected that most civil engineers are most interested in artificial (or man-made) composites. Exceptions might be those who are designing structures to be made out of wood [5, 6].

1.1.1 Macroscopic composites

These typically are composite materials where the individual components are large enough to be seen without the use of a microscope. Some examples of these are concrete (which is a mixture of gravel and cement), steel reinforced concrete (a mixture of steel, gravel, and cement), and laminated wood (which is a mixture of wood with different grain orientations). One should note that a composite could consist of materials of very different type (such as steel reinforced concrete). It can also consist of the same material, with different portions of the material oriented in different directions [7]. Sometimes composites are used together. One example is a fibre/macroscopic composite that are used to hold roadway beams together during earthquakes.

1.1.2 Microscopic composites

Microscopic composites are composed of materials whose individual components are microscopic in scale (but still much larger than the atomic scale).

1.1.2.1 Dispersion strengthened composites

In dispersion strengthened materials, small particles of the order of 10^{-5} to 2.5 x 10^{-4} mm in diameter are added to the matrix material. Up to 15 % by volume of the material can be these particles. These particles act to help the matrix resist deformation. This makes the material harder and stronger. The matrix material is carrying most of the load. The properties of these materials are affected by their texture and microstructure. It is well known that the presence of particles can affect the development of texture during processing. Although this aspect has been studied for alloys reinforced with high volume fractions of ceramics [8, 9, 10], little information is available for alloys reinforced with high volume fractions of inter-metallic phases [11].

A magnesium alloy matrix composite reinforced by a continuous TiNi shape memory alloy (SMA) fibre was fabricated by pulsed current hot pressing (PCHP) of TiNi SMA fibres sandwiched with a pair of AZ31 Mg alloy plates, and its microstructure and mechanical properties were examined. The tensile yield stresses of the composite, deformed in tension at 373 and 423 K, were higher by about 68 and 87 MPa than that at 293 K, respectively. At the test temperature range, both the yield stress and elongation of the composite increased with

increasing temperature. At temperatures higher than 373 K, the specific strength of the composite was higher than that of the AZ31 Mg alloy [12].

Gupta and Srivatsan [13] studied a hybrid composite based on the magnesium alloy AZ91A reinforced with copper particulates, and which was fabricated using the disintegrated melt deposition (DMD) processing technique followed by hot extrusion. Micro-structural characterization of the extruded composite sample revealed a near uniform distribution of the copper particulates and other inter-metallic phases through the magnesium alloy metal matrix, good integrity at the copper–magnesium alloy matrix interfaces and evidence of minimal porosity. Mechanical property quantification revealed that the addition of copper particulates resulted in a significant increase in elastic modulus and ultimate tensile strength of the composite material, and an improvement of 0.2 % in yield strength. However, ductility of the composite was marginally affected when compared to its un-reinforced monolithic counterpart. The overall mechanical properties of AZ91A/Cu composite were found to be higher than the silicon carbide particulate reinforced AZ91 composite, even for higher volume fractions of the particulate reinforcement. Influence of copper in the matrix of magnesium alloy AZ91A was examined in light of intrinsic micro-structural features and mechanical properties of the composite.

The partitioning of stress between bridging and broken fibres and the nearby matrix in the region around a fatigue crack in the matrix of a Ti–6Al–4V/SCS–6 SiC fibre composite was studied [14]. This was achieved by using synchrotron X-ray radiation to perform a combination of high spatial resolution topographic imaging and strain mapping. The contributions of broken and bridging fibres were separated using a double peak fitting routine. The interfacial stress variation and the extent of interfacial de-bonding were deduced from the fibre strain profiles. Contrary to most micromechanical models the interfacial frictional sliding stress was not found to be constant along the fibre length, but it decreased approximately linearly towards the crack plane. Upon unloading, the fibres were found to undergo reverse sliding at the interface.

1.1.2.2 Particle strengthened composites

The particles in these composites are larger than in dispersion-strengthened composites. The particle diameter is typically of the order of a few microns. Typically the particles comprise between 20 % and 40 % (by volume) of the composite. In this case, the particles carry a major portion of the load [15]. The purpose of the matrix is just to hold the

particles together. The original aim of these composites is to combine the merits of different phases in one, i.e., to design materials that have better properties than any one of their components. Such ceramic particle reinforced alloys have improved high temperature strength and creep resistance. Oxide dispersion-strengthened super alloys (ODS) in aerospace application as well as metal matrix composites (MMCs) used in the automotive industry are examples [15].

The wear of sintered diamond tools in the cutting of SiC-particle–epoxy composites was also studied. The effects of the SiC particle size, volume ratio in the composite and diamond grain size of the cutting tool on tool wear were investigated. The experimental work has shown that a coarse-grained diamond tool exhibits higher wear resistance than the corresponding fine-grained tool. Greater tool wear was obtained in cutting the composites that had coarser particles and a higher volume ratio of SiC. Moreover, it was found that the tool wear increases drastically when the SiC particles are larger than the tool grains. A wear model of the tool was proposed, in which the tool is worn mainly by the 'tear-off' mechanism of the diamond grains. This model could explain the experimental results by comparing the pushing force of a SiC particle with the tear-off resistance of the diamond grains of the tool. Finally, a fatigue-like empirical curve was established. This curve was used to predict the wear of the tool during cutting of the composite [16].

A well-dispersed (Ti, Nb, W)C particulate reinforced nickel-base super-alloy was prepared via super-high temperature (above 2123 K) treatment of the melt. Scanning electron microscopic (SEM) observation and energy dispersive X-ray spectroscopy (EDS) results showed that most of the (Ti, Nb, W) C particles have a carbo-nitride core. Gas analysis showed that nitrogen content in the alloy with super-high temperature treatment of the melt is much higher than that in the conventional cast super-alloy. The well-dispersed (Ti, Nb, W)C particles could be attributed to nitrogen combining with Ti in the alloy melt to produce TiN, which acts as the nucleator to form (Ti, Nb, W)C. This work [17] provided a new way to prepare the TiC particulate strengthened composites.

3D finite element calculations comparing to axi-symmetric calculations have been performed to predict quantitatively the tensile behaviour of composites reinforced with ceramic particles aligned in stripes. The analyses were based on a unit cell model, which assumes the periodic arrangement of reinforcements. The results were presented in such a manner that they can be directly compared for all possible aspect ratios and inclusion volume fractions. It was indicated that varying the distance between the stripes when the particle volume fraction was kept constant, significantly influenced the overall mechanical behaviour

of the composites. Whereas during elastic deformation 3D and axi-symmetric formulations predict quantitatively similar results, the mechanical behaviour perpendicular to the stripe direction predicted by 3D and axi-symmetric models differ depending on the inclusion volume fraction. Nevertheless, an appreciable strengthening in the stripe direction independent of the model and deformation stage was predicted [18].

1.1.2.3 Fibre reinforced composites

Fibre reinforced composites are composite materials where fibres have been added to increase the load carrying capability of the material. The fibres may occupy anywhere from 40 to 60 % (by volume) of the material. A typical graphite fibre diameter may be of the order of 5-7 x 10^{-3} mm in diameter [20].

Short fibre composites are probably the easiest type of fibre composite material to make. In this situation the fibres are cut into short pieces (in the order of a few millimeters long). It should be noted that these fibres are still long with respect to their diameter [19]. The fibres are then randomly mixed into the polymeric matrix. This type of composite will tend to have isotropic mechanical properties (which make it easier to design), but it means it is neither as stiff nor as strong as it could be if the fibres were oriented. Complicated cast shapes can be made from this type of composite, if the resin is heated into the liquid region. The presence of the fibres will make it behave like a viscous liquid [20].

One problem with short fibre structures is that most do not exhibit the maximum amount of strength and stiffness that could have been obtained from the fibres. Maximum strength and stiffness in the fibre direction could be obtained if all of the fibres were oriented in the same direction. However, such a lay-out would result in a very weak system transverse to the fibres. This is because a composite loaded transverse to the fibres could fail without having to break any of the fibres. Therefore, it is usually considered desirable to have a variety of fibre orientations in a given structure [21].

Short fibre reinforced thermoplastics (SFRT) are potential structural materials because of their capability of being easily transferred into complex shapes by injection molding, and their much better mechanical property profile in comparison to un-reinforced polymers. Polytetrafluoroethylene (PTFE) is one of the candidate matrices, especially if the advantages of chemical and thermal oxidation resistance as well as a good lubrication ability are required, e.g. for tribological applications in severe environments. The poor mechanical properties of a durable semi-crystalline thermoplastic polymer with unattractive mechanical properties, like

PTFE, can be improved by blending it with a hard and strong polymer phase, such as polyetheretherketone (PEEK). Short carbon fibres (CF) are used to increase the creep resistance and the compressive strength of the polymer matrix system. A series of PTFE based composites with different amounts of PEEK and CF were considered [22].

Knowledge of the dynamic mechanical properties of fibre composites is of importance when considering energy dissipation processes in cyclic loading applications. Viscoelasticity is one typical property of polymeric materials, and it plays also an important role in polymer-based composites. Viscoelasticity can be investigated by dynamic experiments, in which the dynamic storage modulus and damping (loss factor) are two important linear viscoelastic parameters. The storage modulus corresponds to the stiffness of the material under dynamic loading. The complexity of damping mechanisms in fibre composites can be considered in two categories, low-strain and high-strain damping. Low-strain damping is a domain of the polymeric matrix which obeys linear viscoelastic relations. High strains induce micro-cracks, which contribute to damping by friction. In addition, the fibre-matrix interface strongly affects the mechanical properties of the composite and also has an influence on its damping level. Interfacial bonding in fibre-reinforced composites can be considered as weak, ideal or strong. An ideal interface plays the role of transferring loads, but does not contribute to damping. However, under normal conditions interface damping must also be considered in practical applications [23].

It is well known that lightweight fibre-reinforced polymer composite materials have higher specific strength and stiffness when compared with conventional structural materials such as metals. Much effort has been devoted to the improvement and optimization of these properties as pertaining to various classes of composite microstructures. Good vibration damping properties are also particularly important for composite structures when they are used under dynamic loading, e.g. in aerospace structures. Due in part to the extensive accumulated experience with conventional structural materials, such as metals, which in general have poor internal damping, the potential for the improvement and optimization of damping in fibre-reinforced composites has not yet been fully realized. Meanwhile, the full use of discontinuous fibre-reinforcement has not yet been fulfilled in composite material applications. This may be due to the direct accomplishment of higher specific strength and stiffness in the more familiar continuous fibre composites [24].

Wood fibre reinforced polypropylene composites of different fibre content (40, 50 and 60 % by weight) have been prepared and wood fibres (hard and long fibre) were treated with compatibiliser (MAH-PP) to increase the interfacial adhesion with the matrix, to improve the

dispersion of the particles and to decrease the water sorption properties of the final composite. Results indicated that impact properties were affected by moisture content. The Charpy impact strength decreased and maximum force was increased with increasing of moisture content. With the addition of MAH-PP (5 % relative to the wood fibre content), the damping index decreased around 145 % for hard wood fibre–PP composites at 60 wt.% wood fibre. Long wood fibre–PP composites showed more impact resistance than hard wood fibre–PP composites. Short-term flexural creep tests were conducted to investigate the creep behaviour of wood fibre–PP composites. Three experimental parameters were selected: the addition of compatibiliser, temperature and wood fibre content. The addition of MAH-PP increased creep modulus, that means it reduced the creep. The extent of creep resistance (creep modulus and creep strength) decreased with increasing temperature. It was also found that wood fibre content has a great effect on creep resistance, which is increased with increasing wood fibre content [25].

The mechanical behaviour of high-density polyethylene (HDPE), reinforced with continuous henequen fibres (*Agave fourcroydes*), was studied. Fibre-matrix adhesion was promoted by fibre surface modifications using an alkaline treatment and a matrix pre-impregnation together with a silane coupling agent. The use of the silane coupling agent to promote a chemical interaction, improved the degree of fibre-matrix adhesion. However, it was found that the resulting strength and stiffness of the composite depended on the amount of silane deposited on the fibre. A maximum value for the tensile strength was obtained for a certain silane concentration, but when using higher concentrations, the tensile strength did not increase. Using the silane concentration that resulted in higher tensile strength values, the flexural and shear properties were also studied. The elastic modulus of the composite did not improve with the fibre surface modification. The elastic modulus, in the longitudinal fibre direction obtained from the tensile and flexural measurements, was compared with values calculated using the rule of mixtures. It was observed that the increase in stiffness from the use of henequen fibres was approximately 80 % of the calculated values. The increase in the mechanical properties ranged between 3 and 43 %, for the longitudinal tensile and flexural properties, whereas in the transverse direction to the fibre, the increase was greater than 50 % with respect to the properties of the composite made with untreated fibre. In the case of the shear strength, the increase was of the order of 50 %. From the failure surfaces it was observed that with increasing fibre-matrix interaction the failure mode changed from interfacial failure to matrix failure [26].

1.1.2.4 Hybrid composites

Hybrid composites are composites that are a mixture of more than two different types of materials. An example of a hybrid composite would be steel reinforced concrete (which has a mixture of steel, gravel, and cement). A hybrid fibre-based composite could be one that is composed of an epoxy resin, carbon fibres, and glass fibres. A hybrid composite could also be a mixture of particle and fibre reinforcement. An example of this has been used with graphite/epoxy systems. The epoxy resin is rather brittle. In an effort to make the resin more ductile, some engineers have added rubber particles to the resin. These particles bond poorly with the resin, and act to form dull cracks (which can be used to resist crack growth). This might be called particle weakening rather than particle strengthening. The fibres are in this system to make it strong, and the rubber particles are added to the resin to make it more ductile [27]. Mechanical properties of unidirectional high-performance polyethylene (HP-PE) fibre-carbon fibre-epoxy resin hybrid composites were studied, emphasizing tensile, compressive and shear strengths, initial and long-term moduli, vibrational damping, and impact response. The stiffness and compressive strength of the composites varied linearly with HP-PE fibre content, but improved adhesion of HP-PE fibres had no effect on the composite modulus or compressive strength. Shear strength increased with increasing HP-PE fiber-epoxy resin adhesion and decreasing HP-PE fibre content. Storage and loss moduli varied linearly with HP-PE fibre content. Damping increased rapidly with HP-PE fibre content. Improved adhesion of HP-PE fibres resulted in lower impact energies due to failure modes that are strongly altered from a more ductile to a more brittle character [28].

Al_2O_3 and/or carbon short fibre reinforced Al–12Si alloy composites were prepared by a pre-form squeeze-infiltration route. High temperature friction and wear properties of the composites were investigated [29] at a constant sliding velocity of 1.57 $m.s^{-1}$ and a load of 50 N as well as a sliding distance of 942 m. Worn surfaces and sub-surface regions were also analysed. The results show that the hybrid composites reinforced with Al_2O_3 and carbon fibres attained superior wear resistance over the entire range of test temperatures. Compared with the monolithic alloy, the critical transition temperature from mild wear to severe wear of 12 vol.% Al_2O_3/Al–12Si composites improved markedly between the ranges 150–200 and 250–300 °C. The addition of 4 vol.% C in the 12 vol.% Al_2O_3/Al–12Si composites further improved the critical temperature to a range between 350 and 400 °C. The friction coefficient of the hybrid composites containing a fixed 4 vol.% C increased with Al_2O_3 fibre volume fraction up to 20 vol.%, except at 300 °C the trend reversed for 4 to 12 vol.% Al_2O_3.

However, there existed an optimum range of Al_2O_3 fibre volume fraction leading to the least wear rate of the hybrid composites containing a fixed 4 vol.% C. The friction coefficient and wear rate of the hybrid composites containing a fixed 12 vol.% Al_2O_3, decreased with the increase of carbon fibre volume fraction up to 6 vol.%. Analysis of worn surfaces and subsurface regions indicated that the reinforcing fibres have no significant effect on the wear mechanisms of the Al–12Si alloy. The dominant mechanisms were cutting grooves and de-lamination, as well as slight adhesion in the mild wear regime. The dominant wear mechanisms shifted to severe adhesion at test temperatures above the critical transition temperature.

1.1.3 Examples of continuous fibre reinforced composite materials

1.1.3.1 Composites composed only of fibres

This type of composite usually has the fibres woven into some cloth type structure. Rather than having the resin holding the fibres together, the nature of the woven pattern holds the fibres together. The most notable example of this type is carbon–carbon composites. These composites consist of a woven carbon fabric. This composite is usable for very high temperature applications (since carbon has a very high melting temperature). This type of composite is rather expensive, and is usually only used in very high temperature applications. It may also be porous to liquids, making it of doubtful usability in dam and lock structures [30].

1.1.3.2 Metal matrix composites

Metal matrix composites are used in high temperature applications where a traditional polymeric matrix would not work. One example of this type would be boron-aluminum. This type is also rather expensive and not likely to be used in civil engineering applications where high temperature is not a problem [31].

1.1.3.3 Polymeric matrix composites

Polymeric matrix composites are composites consisting of fibres immersed in a polymeric matrix. These are much cheaper than the two fibre composite types discussed

above. Within this group there are many different types of resin and fibre that could be chosen.

Generally composites are formed from two or more types of materials. Examples include polymer-ceramic and metal-ceramic composites. They are used because overall properties of the composites are superior to those of the individual components. For example: polymer-ceramic composites have a greater modulus than the polymer component, but are not as brittle as ceramics. Composites are also found in nature. Wood, a natural composite containing cellulose fibre, is one of the most common materials used in the construction industry [32].

1.2 Fillers

In recent years fillers in polymers have come to play an increasingly functional role. Addition of mineral fillers was common practice for improving the cost/performance balance of polyolefins, with particular reference to the increase of stiffness and temperature resistance, and to the reduction of creep, shrinkage, warpage, and thermal expansion. In general, it can be stated that the mechanical properties, and in particular impact strength and toughness, can be drastically varied, depending on matrix characteristics, type, and content of filler, and the adhesion between filler and matrix [33]. As a result, considerable efforts have been made to find suitable reinforcing fillers. Particulate inorganic fillers are commonly added to commercial thermoplastic resins to achieve economy as well as to favourably modify certain properties such as stiffness, heat distortion and moldability [34].

Recently, cellulosic fillers of fibrous nature have been of great interest, as they can yield composites with improved mechanical properties compared to those containing non-fibrous fillers [35]. When used as reinforcing agents for composites, they offer a number of benefits when compared with mineral fillers, i.e. high specific stiffness and strength, desirable fibre aspect ratio, flexibility during processing with no harm to the equipment, low density, biodegradability and finally, low cost per unit volume basis. Several cellulosic products and wastes such as shell flour, wood flour and pulp have been used as fillers in thermoplastics [35, 36]. Additionally, the properties of cellulosic fibres compare favourably with other reinforcing fibres that are commonly used [37]. Natural fibres are much cheaper than synthetic fibres and could replace synthetics in many applications where cost savings outweigh strength requirements [38]. They are subdivided based on their origin, whether coming from plants, animals or minerals. Plant fibres may include hairs (cotton, kapok), fibre

sheafs of dicotylic plants or vessel-sheafs of monocotylic plants, i.e. bast (flax, hemp, jute, ramie), and hard fibres (sisal, henequene, coir) [39, 40].

Sisal fibre is one of the most widely used natural fibres and is very easily cultivated. It has short renewal times and grows wild in the hedges of fields and railway tracks. Nearly 4.5 million tons of sisal fibre is produced every year throughout the world. Tanzania and Brazil are the two main producing countries [41]. Sisal fibre is a hard fibre extracted from the leaves of the sisal plant (*Agave Sisalana).* Though native to tropical and sub-tropical North and South America, the sisal plant is now widely grown in tropical countries of Africa, the West Indies and the Far East [42].

The fibre properties and fibre structure are influenced by several conditions and vary by area of growth, its climate and the age of the plant. Further, the technical digestion of the fibre is another important factor which determines the structure as well as the characteristic properties of the fibres [43]. The length of the fibre should be above a critical value for effective stress transfer from the matrix to the fibre, which in turn depends on the bonding between the fibre and matrix. The higher the bond strength, the lower the critical length and *vice versa.* Similarly, the reinforcing effect of the fibres at low volume fraction is pronounced only when good interfacial bonding exists between the fibre and matrix [41, 42].

Mechanical performance of a fibre reinforced plastic composite primarily depends on three factors: (a) strength and modulus of the fibre, (b) strength and chemical stability of the resin, and (c) effectiveness of the bond between resin and fibre in transferring stress across the interface [39]. Many of the properties of fibrous composite materials are strongly dependent on micro-structural parameters such as fibre diameter, fibre length, volume fraction of fibres, and alignment and packing arrangement of fibres. In randomly oriented short fibre composites, the fibre length and content play an important role in determining their mechanical performance [36].

The tensile properties of sisal fibre are not uniform along its length. The root or lower part has low tensile strength and modulus, but high fracture strain. The fibre becomes stronger and stiffer at mid-span and the tip has moderate properties. Mukherjee and Satyanarayana [44] studied the effects of fibre diameter, test length and test speed on the tensile strength, initial modulus and percent elongation at break of sisal fibres. They concluded that no significant variation of mechanical properties with change in fibre diameter was observed. However, the tensile strength and percent elongation at break decrease, while Young's modulus increases with fibre length. With increasing speed of testing, Young's

modulus and tensile strength both increase, but elongation does not show any significant variation. Yang *et al.* [45] used IR, X-ray diffraction and thermogravimetry (TG) to study the effect of thermal treatment on the chemical structure and crystallinity of sisal fibre. They found that the IR spectrum did not change below 200 °C treatment, while density and crystallinity increased. This means that the chemical structure of sisal fibres will not change below 200 °C while the degree of crystallinity can increase and hence the density. There was a slight weight loss (≈ 2%) below 200 °C, probably caused by the evaporation of water absorbed by sisal fibre, substances of low boiling point and others that can be decomposed below this temperature. They also found that thermal decomposition of sisal fibre could be divided into three stages. The thermal behaviour is essentially identical for heat treatment between 150 and 200 °C. Hence, thermal treatment of sisal fibre can be carried out below 200 °C.

Several types of polymers have been used as matrices for natural fibre composites. The most commonly used are thermoset polymers such as polyester, epoxies and phenolics. Thermoplastics like polyethylene, polystyrene, and polypropylene have also recently been used as matrices. These polymers may have different affinity towards the fibre due to differences in their chemical structure. As a consequence, the reinforcement effect of the fibres in these matrices may vary widely. It is well known that some polymers are susceptible to reinforcement, while others are not with respect to a particular filler. For fibre filled composites it has been reported that the higher the flow limit of the matrix, the lower the critical length of the fibre [40]. This means that, for example, the fibres used to reinforce polyethylene have a critical length 4-5 times higher than those used for the reinforcement of nylon or polyacetal resins. However, very few studies have been reported in literature on the use of sisal fibre as reinforcement in thermoplastic polymers like low-density polyethylene (LDPE) and thermosetting polymers like epoxy and phenol-formaldehyde [36].

1.3 Surface modification

Incorporation of fibres (man-made or natural) into a polymer is known to cause substantial changes in the mechanical properties of composites. A good interfacial bond between fibre and matrix can substantially improve the mechanical properties of the composites. Interfacial shear strength is one of the means of determining bonding between fibre and matrix. The term "interface" has been defined as the boundary region between two

phases in contact. The composition, structure or properties of the interface may be variable across the region and may also differ from the composition, structure or properties of either of the two contacting phases [46]. This interfacial region exhibits a complex interplay of physical and chemical factors that exerts a considerable influence on and control over the properties of reinforced or filled composites.

The problem encountered when attempting to combine plant fibres or lingo-cellulosic material with a thermoplastic or thermoset matrix, is one of incompatibility. The reason for this is due to the abundant hydroxyl functionality of fibre cell wall polymers, which ensures that the material is hydrophilic. Generally thermoset, thermoplastic or elastomer polymers are almost all hydrophobic. The problem then is of 'wetting' the fibre [46].

Several investigators [47, 48] studied the surface morphology, as well as mechanical and degradation properties, of the treated fibres. Yang *et al.* [47] studied the relationship of surface modification and tensile properties of sisal fibres. Their modification methods include: alkali, H_2SO_4, conjoint H_2SO_4 and alkali, benzol/alcohol de-wax, acetylated, thermal, alkali-thermal, and thermal-alkali treatments. Thermal treatment seems to be the most desirable method in terms of strength and modulus properties, because of the increased crystallinity (from 62.4 % for untreated to 66.2 % for 150 °C / 4 h treated) of sisal fibres. Other treatments increase the ductility of sisal fibres substantially, but decrease the modulus.

Oil palm fibres have been found to be an excellent reinforcement in phenolic matrices. A detailed investigation on the water sorption characteristics of oil palm fibres was carried out. Various fibre surface modifications such as mercerization, latex coating, gamma irradiation, silane treatment, isocyanate treatment, acetylation and peroxide treatment were tried to reduce the hydrophilicity and thereby decreasing the sorption characteristics. The effects of treatments on the sorption characteristics of oil palm empty fruit bunch fibre in distilled water at four different temperatures were investigated. Changes in physical and chemical modifications of fibres upon different treatments changed the water sorption behaviour. Treatment reduced overall water uptake at all temperatures. Hydrophilicity of the fibres decreased upon many modifications, which decreases water uptake. The effect of sorption on the mechanical performance of the treated and untreated fibres was also investigated. It was found that the mechanical properties of the fibres decrease upon sorption and regains on desorption [49].

In the study of the modification of natural fibre with acetic anhydride, it was reported that the reactivity of the fibre cell wall with acetic anhydride is in the order of lignin > hemi-

cellulose > cellulose. The reactivity is dependent upon the relative reactivities of the hydroxyl group in the substrate [50], and the rate of diffusion of the reagent into the fibre matrix [51]. Kapok/cotton fabric was used as reinforcement for conventional polypropylene and maleic anhydride grafted polypropylene resins. Treating the reinforcement with acetic anhydride and sodium hydroxide modified the fabric (fibres). Thermal and mechanical properties of the composites were investigated. Results showed that fibre modification gives a significant improvement in the thermal properties of the plant fibres, whereas tests on the mechanical properties of the composites showed poor tensile strength. Mercerisation and weathering were found to impart toughness to the material, with acetylation showing slightly less rigidity compared to other treatments on either the fibre or composites. The modified polypropylene improved the tensile modulus and had the least toughness of kapok/cotton reinforced composites. Maleic anhydride isotactic polypropylene (MAIPP) reinforced with plant fibres gave better flexural modulus at lower fibre content compared with glass fibre reinforced MAIPP [52].

The mechanical properties of sisal fibre composites (randomly oriented) of several thermoset resin matrices (polyester, epoxy, phenol-formaldehyde) and a thermoplastic matrix (low density polyethylene (LDPE)) were evaluated with respect to fibre length and fibre loading [36]. All the composites showed a general trend of increase in properties with fibre loading. However, the optimum length of the fibre, required to obtain an increase in properties, varied with the type of matrix. Among polyester, epoxy and phenol-formaldehyde composites of sisal fibre, a phenolic type resin performed as a better matrix than epoxy and polyester resins with respect to tensile and flexural properties, due to the high interfacial bonding in phenolic composites. However, when compared to thermoset resin composites, sisal fibre-LDPE composites showed a better reinforcing effect due to the high matrix ductility and high strength/modulus ratio of sisal as compared to that of the LDPE matrix [36].

1.4 Biodegradable polymers

Biodegradable polymers have been the subject of research and development since the early 1970s and growing pressure on the world's resources as well as concerns about disposal of plastics led to intensified interest and commercial activity in the 1990s. Biodegradable polymers, or biopolymers as they are sometimes known, are now attracting interest for a wide range of applications from special high-performance products, medicine and surgical

applications through to commodity uses in films and packaging [53]. The current biodegradable polymers may be divided into synthetic and natural polymers, while the latter are classified into those of plants and microorganisms. The degradation of such polymers includes the disintegration into their monomers. Therefore unstable and hydrolysable linkages are required, where chemical, biological or photochemical reactions take place. Some polyesters (e.g. poly-β-hydroxyl butyrate) and polysaccharides like thermoplastic starch or modified cellulose are well suited for that purpose.

On the one hand, water solubility raises the degradability, but on the other, in most cases a water-resistant material should be obtained for most applications. This problem can be avoided by blending soluble polymers like thermoplastic starch with insoluble polyesters, which additionally show very good manufacturing properties [54].

The growing environmental awareness and new rules and regulations are forcing the industries to seek more ecologically friendly material for their products. For example, automotive applications based on natural fibres with polypropylene as matrix material are very common today. Less work has been done to study composites with matrices, which originate from renewable raw materials, for example poly-lactic acid, cellulose esters, poly-hydroxyl butyrate, starch and lignin based plastics. The problems with these polymers have been poor commercial availability, poor processability, low toughness, high price and low moisture stability. The long-term properties of renewable materials are also very important, especially if the products are not single use applications [55]. Poly-L-lactic acid (PLLA), the most popular biodegradable polymer due to ecological reasons, was used as the matrix resin. It is a synthetic high polymer originating from natural products and it has a relatively high melting point (usually around 60 °C) and good mechanical performance (56). The degradation occurs by hydrolysis to lactic acid, which is metabolized by microorganisms to water and carbon monoxide. By composting together with other biomass the biodegradation occurs within two weeks, and the material has fully disappeared within 3-4 weeks [57].

If biodegradable polymers are reinforced with de-gummed fibres, these materials have sufficient mechanical properties to be used as lightweight construction materials. In particular bast fibres, such as hemp or flax, are suitable for polymer reinforcement without the loss of the material's biodegradability. Their weight specific mechanical properties are comparable to those of glass fibres [54].

1.5 Sisal fibre-rubber composites

In recent years, short fibre reinforced elastomers have gained wide importance due to the advantages in processing and low cost coupled with high strength. Many researchers used short glass fibres for reinforcing rubbers because of their high modulus, high strength and low creep. Moreover, reinforcement with short fibres offers some attractive features such as high modulus and tear strength. Major factors that affect the performance of rubber-fibre composites are fibre loading, fibre dispersion, fibre orientation, fibre to matrix adhesion and the aspect ratio of the fibre. These materials bridge the gap between conventional elastomers and fibres by combining the stiffness of short fibres with the elasticity of rubber. The major applications of these composites are in tyre treads, roofings, hoses, sheetings, V-belts, industrial rubber products and complex shaped articles [58].

The increasing use of short fibre composites in static and dynamic applications led to the importance of stress relaxation measurements, since the behaviour of the rubber-fibre interface can be easily detected by stress relaxation studies. Vulcanized rubbers, when subjected to constant deformation, decay in stress by an amount proportional to the logarithm of the period in the deformed state. The stress relaxation behaviour of short jute fibre-reinforced nitrile rubber composites with respect to the effect of strain level, bonding agent, fibre content, fibre concentration, temperature and pre-strain on the relaxation behaviour has been studied in detail by Bhagawan *et al.* [58]. They concluded that in general, short fibres increase the rate of stress relaxation over the corresponding unfilled vulcanizate. Composites, containing a bonding agent, exhibit slower relaxation than those without a bonding system, and the effect of fibre orientation on the relaxation behaviour appears to be marginal. Pre-strain decreases the stress relaxation rate considerably, particularly for composites without bonding agent. Varghese *et al.* [59] studied the stress relaxation behaviour of acetylated short sisal fibre reinforced natural rubber composites, with special reference to the effects of strain level, fibre loading, bonding agent and temperature. They reported the existence of a single relaxation pattern in the unfilled stock, and a two-stage relaxation mechanism for the acetylated fibre filled natural rubber composites. It was also observed that, for the composites in the absence of bonding agent, the rate of relaxation increased with strain level, but in the presence of bonding agent, the relaxation rate is almost independent of strain level, because of the strong fibre-matrix interface.

However, studies on composites containing plant fibres are important because of the renewable nature of the plant fibres, their low cost and amenability to chemical and

mechanical modifications. A considerable amount of research work was reported on plant fibre reinforced elastomer composites [59, 60, 61]. They studied the properties of cellulosic fibre-elastomer composites and found that the aspect ratio of the fibre plays a major role in composite properties.

The effects of particulate fillers on cellulosic fibre-elastomer composites have also been reported. It was found that fibre-matrix adhesion in the silica-carbon black system could be promoted by the addition of definite proportions of silica/resorcinol/hexamethylene tetramine, and that the addition of either carbon black alone or both silica and carbon black to a rubber compound containing resorcinol and hexamethylene tetramine, gave rise to good adhesion between the fibre and rubber matrix, and that the silica carbon black system exhibit an improved adhesion. It was also reported that processing properties like green strength and mill shrinkage were improved by the addition of fibre, and that fibre addition also improved the tear strength by obstructing the development of the tear path [62].

Prasant and Thomas [63, 64] investigated the processing behaviour and mechanical properties of short sisal fibre reinforced styrene butadiene rubber (SBR) composites. Tear strength was examined with special reference to the effects of fibre length, fibre orientation, fibre concentration and bonding agent. It was observed that an increase in the concentration of fibre increases the tear strength in both longitudinal and transverse directions. It was also found that the tear strength values were almost three to four times higher than those of the unfilled vulcanizates under similar conditions. They have determined the green strength, mill shrinkage and Mooney viscosity of the composites to analyze the processing behaviour.

1.6 Sisal fibre-thermoset composites

Incorporation of sisal fibre into thermoset plastics was reported by various workers [65, 66, 67, 68]. Paramasivam and Abdulkalam [65] investigated the feasibility of developing polymer-based composites using sisal fibres due to the low cost of production of the composites, and the amenability of these fibres to winding, laminating and other fabrication processes. It was found that the fabrication of these composites was fairly easy and the cost of production was quite low. Winding of cylinders with longitudinal or helical and hoop reinforcement was successfully carried out. The tensile strength of sisal epoxy composites was found to be 250-300 MPa, which was nearly half the strength of fibre glass-epoxy composites of the same composition. Because of the low density the sisal fibre, however, the specific strength of sisal composites was comparable with that of glass composites. The

unidirectional modulus of sisal-epoxy composites was found to be about 8.5 GPa. This study indicated the feasibility of developing composites incorporating one of the abundantly available natural fibres, to be used in the field of consumer goods, low cost housing and civil engineering structures.

Satyanarayana *et al.* [54] studied the mechanical properties of chopped sisal fibre–polyester composites. Chopped sisal fibre-polyester composites were prepared by a compression molding technique. It was found that the specific modulus of the composite was 1.90 GPa compared with 2.71 GPa for glass fibre reinforced plastics, while the specific strength was of the same order as that of polyester resins (34 - 41 MPa). The impact strength was 30 J m^{-2}, which is three times higher than that of polyester and 30 % less than glass fibre reinforced plastics. Accelerated testing revealed little change in the initial modulus, and reductions of 5 % in ultimate tensile strength, 16 % in flexural strength and 5.4 % in water absorption were observed.

Pavithran *et al.* [66, 67] reported on the impact properties of oriented sisal fibre-polyester composites. Unidirectionally aligned sisal fibre-polyester composites containing 0.5 volume fraction of sisal fibre were prepared from unsaturated polyester pre-pregs. The impact strength of the composites was measured by the Charpy test in a pendulum impact-testing machine using a pendulum load of 0.4 kg. They compared the work of fracture of sisal fibre-polyester composites to those of composites containing other natural fibres. It was seen that sisal fibre composites had the maximum work of fracture followed by pineapple fibre composites. Banana and coir fibre composites had a comparatively low work of fracture. It is a generally accepted fact that the toughness of a fibre reinforced composite is mainly depending on the fibre stress-strain behavior. Strong fibres with high failure strain impart high work of fracture on the composites. Among sisal, pineapple and banana fibre reinforced polymer composites, sisal fibre-polyester composites is likely to give high work of fracture because of the high toughness of sisal fibre which is found in agreement with the experimental results. Banana and pineapple fibres had comparative mechanical properties, but the large difference observed in the work of fracture of their composites was not explained. The coir composites were expected to give high toughness due to the high toughness of the fibre. However, a low value was observed. They also studied the variation in impact properties of various natural fibre composites with micro-fibrillar angle of the fibre. They observed an influence of micro-fibrillar angle of the fibre on the work of fracture values of different natural fibre reinforced polymer composites. Micro-fibrillar angle in plant fibres plays an important role in determining the impact behaviour of these composites, and this

effect should be taken into account along with the other parameters while predicting the impact properties of natural fibre composites.

Pavithran *et al.* [67] compared the impact properties of unidirectionlly oriented sisal fibre-polyester composites with those of composites having ultra high-density polyethylene (UHDPE) and glass fibres. It was observed that sisal composites show work of fracture identical with that of ultra high-modulus polyethylene composites, and the toughness of sisal fibre composites is only 25 % less than that of glass fibre composites when the density of the latter is taken into account. The high work of fracture obtained for the sisal fibre composites, in spite of the fibre having low strength and modulus, confirms their earlier argument that the prediction of impact behaviour of natural fibre composites will not be valid unless the contribution from the helically wound micro-fibrillar structure of the fibre is taken into account. It is generally accepted that the toughness of a fibre composite is mainly dependent on the fibre stresss-train behaviour. Strong fibres with high failure strain impart high work of fracture on the composites.

Bisanda and Ansell [70] studied the effect of silane and alkali treatment on the mechanical and physical properties of sisal-epoxy composites. They reported that incorporation of sisal fibres in an epoxy resin produces stiff and strong composite materials. The treatment of the sisal fibres with silane, preceded by mercerisation, provides improved wetability, mechanical properties and water resistance.

1.7 Sisal fibre-thermoplastic composites

Thermoplastic polymers constitute an important class of materials with a wide variety of applications. Because of its increasing use, combined with high demand, the cost of the polymeric raw material has increased rapidly over the past decade. This situation made it necessary to use low cost fillers as means of reducing the cost of the end product. However, the widely used inorganic fillers, such as glass fibre and mica are very expensive compared to wood fibres.

Several cellulosic products and wastes such as shell flour, wood flour and pulp have been used as fillers in thermoplastics [71, 72, 73]. Raj *et al.* studied the influence of wood flour on the mechanical properties of polypropylene [74], and they found that the cost of material could be reduced without too much loss of elastic modulus. However, fibrous fillers are now gaining more importance over particulate fillers due to their high performance in mechanical properties. Published data show that various commercial wood fibres have good

potential as reinforcements in thermoplastics. Wood fibres are non-abrasive so that relatively large concentrations of fibres can be incorporated into polyolefins without causing serious machine wear during mixing and processing.

There were also studies [75] on the mechanical properties of wood fibre filled medium density polyethylene (MDPE) composites. They observed a significant increase in modulus with increase in filler content. Very few studies, however, have been reported in the literature on the use of sisal fibre as a reinforcing agent in thermoplastic matrices. Joseph *et al.* [76] investigated the mechanical, rheological, electrical and viscoelastic properties of short sisal fibre reinforced LDPE composites as a function of processing method, fibre content, and fibre length and orientation. The viscoelastic and rheological properties of of these composites were investigated. They reported that longitudinally oriented composites showed maximum storage moduli and a critical fibre length of 6 mm is necessary to obtain maximum dynamic moduli. They also reported that fibre damage, that normally occurs during blending of the fibre and the polymer by a melt mixing method, can be avoided by adopting a solution mixing procedure. The unidirectional alignment of the short fibres achieved by an extrusion process enhanced the tensile strength and modulus of the composites along the axis of the fibre alignment by more than two fold compared to randomly oriented fibre composites. They compared the experimentally observed tensile properties (tensile strength and modulus) of short sisal fibre reinforced LDPE composites with the existing theories of reinforcement [77]. They concluded that the tensile properties of short fibre reinforced composites strongly depend on fibre length, fibre loading, fibre dispersion, fibre orientation and fibre matrix interfacial bond strength.

The influence of short glass fibre addition on the mechanical properties of short sisal fibre reinforced LDPE composites have been reported by Kalaprasad *et al.* [77]. They observed that the addition of a small volume fraction of short glass fibre into the above system enhanced the tensile strength of longitudinally oriented composites by more than 80 %. It was also observed that the water absorption tendency of the composite decreases with the process of hybridization.

The electrical properties of coir fibre and sisal fibre reinforced LDPE composites have been studied by Paul and Thomas [78] and Paul *et al.* [79]. They noticed that the dielectric constant of sisal-LDPE and coir-LDPE progressively increases with increase in fibre loading at all frequencies ranging from 1 to 107 Hz. The effect of environmental influences on the mechanical properties of sisal fibre reinforced polymer composites was studied [80]. Dependences between moisture, acid and alkali attacks were determined and the mechanical

properties of sisal fibre-polypropylene were evaluated. They concluded that the bending properties of sisal fibre-polypropylene composites were sensitive to environmental attack. LeThi *et al.* [81], in their studies of the mechanical properties of sisal fibre reinforced polypropylene composites prepared by reactive extrusion, reported that the grafting of the fibres by PP-graft-MA enhanced both the impact strength and the breaking stress of the composites.

The influence of sisal fibre content and different concentrations of dicumyl peroxide (DCP) on the thermal, mechanical and viscoelastic properties of short sisal fibre-linear low-density polyethylene (LLDPE) composites was investigated. Addition of low concentrations (1%) of curing agent (DCP) to the composites prepared by mechanical mixing and subsequent melt pressing of LLDPE and milled sisal fibres, significantly improved their tensile and viscoelastic properties. Composite samples with 1 % DCP have 70 % higher strength than the untreated ones with the same amount of fibre. This is a consequence of peroxide induced grafting between the hydrophobic PE matrix and hydrophilic fibres, which improves their otherwise poor adhesion. Stress relaxation measurements showed that grafting reduces the degree of permanent deformation of the composites, while they are stretched for longer times at a constant strain. However, high DCP concentration (3 %) also induces degradation of the matrix at low sisal contents (< 30 %). This is why these samples show higher stress relaxation rates during prolonged loadings than their untreated counterparts [82].

The variations produced on the mechanical, morphological and thermal properties and on the melt index (MI) of a composite of polypropylene and wood flour (WF) by the modification of the filler were studied. The filler was treated with sodium hydroxide at different immersion times and with vinil-tris-(2-methoxyethoxy)-silane. Polypropylenes functionalized with maleic anhydride (maleated polypropylene, MAPP) were also used as compatibilizers. All the treatments showed the same tendency to slightly increase tensile modulus and tensile strength of the composites, but they did not affect their MFI. Morphological studies showed that the MAPP and silane improved the polymer–WF adhesion and the dispersion of the particles, while the alkaline treatment only improved the dispersion. The silane-modified samples and the use of MAPP produced samples with lower water absorption than those of untreated WF composites. The addition of the filler and the treatments carried out on it caused an increase in the crystallization temperature [83].

The effect of peroxides (dicumyl peroxide and dibenzoyl peroxide) treatment on the tensile properties of sisal fibre-reinforced LDPE composites at 30 % fibre loading was investigated [48]. The tensile values of the composites increase with an increased in

concentration of peroxide up to a certain level (4 % for DCP and 6 % for BP) and then remained constant. This concentration was defined as the critical peroxide concentration at which the tensile strength reaches a maximum for a given fibre content. It was clearly seen from the results that DCP has a lower decomposition rate than BP, and therefore ensures better dispersion in the polymer matrix. This was more efficiently utilized for the grafting reaction between LDPE and cellulose. From the SEM photomicrographs of the tensile fracture surfaces of DCP and BP treated sisal fibre-LDPE composites it was found that PE is grafted onto the cellulose surface. A similar type of peroxide induced PE grafting onto cellulose fibre was reported by Sapieha *et al.* [89]. The treated fibres adhered well to the polymer matrix and underwent breaking and delamination during tensile failure, whereas untreated fibres were easily pulled from the matrix during tensile failure. From the fracture surfaces of DCP and BP treated composites, it was concluded that the interfacial bonding is stronger in the DCP system. Generally, peroxide treated composites showed an enhancement in tensile properties due to the peroxide induced grafting.

1.8 Ethylene vinyl acetate (EVA) copolymer

Ethylene vinyl acetate copolymer has several industrial applications, such as corrosion protection, electrical insulation and manufacture of adhesives, including hot melts. There has been an impressive amount of research on the stability characteristics of EVA-based materials. Various formulations containing vinyl acetate in polyethylene matrix are susceptible to changes in their crystallinity as well as other physical and chemical features, of which the resistance to thermal and radiation damage are the most important [84].

It has been widely used for utensil manufacture due to its mechanical properties. Its properties depend on the vinyl acetate content in the main chain, and also on the polymerization process. When the percentage of vinyl acetate is in the range of 0-45 %, the polymerization process is normally in bulk, the molecular weight is low and the crystallinity is higher than that obtained by a solution process. It is known that the fundamental properties are closely linked to the structure. Hence, the correlation between structure and properties is a good way to get a better characterization of a polymer [85]. Stael *et al.* [86] used nuclear magnetic resonance spectroscopy to obtain further information on the EVA structure. A comparison between magic angle spinning (MAS) and CP/MAS spectra is able to show the presence of different domains or micro-domains in a sample. The variable contact-time experiment permitted them to observe distinct regions that have different mobilities. Their

purpose was to characterize the EVA as a matrix to mix with natural fibres obtained from sugar cane. NMR was used and it allowed them to obtain information on both chemical structure and molecular mobility.

A study of the interface in polymer blends gives the user full information about the thermodynamic miscibility of the system. Surface tension studies of the pure copolymers shoed that the acetate content plays a major role and this is also reflected in the interfacial tension of the PVC blends. The results on surface phenomena and polymer miscibility of PVC/EVA blends [87] show direct relationship between the interface thickness and the vinyl acetate content in the EVA copolymer. Interaction parameter values show an inversely related correlation. Calculated values obtained from the appropriate equations showed small discrepancies from experimental data. The Flory-Huggins parameters, theoretically calculated by using recent theories and which suppose that the vitreous transition is a true transition, are in good agreement with the values obtained from calorimetric measurements. Thermal stability and the degradation process were also studied [87]. The experimental data showed a relationship between the thermogravimetric curves and the degree of interaction in the mixtures as compared to pure polymers that are consistent with microscopy analysis.

EVA polymers could also be a feasible possibility as a resin matrix, although its low mechanical properties could restrict the use of EVA-based composites. Nevertheless, due to the high flexibility presented by the EVA copolymer, EVA-based composites could present some advantages under impact conditions, where toughness plays an important role. The impact performance of chopped bagasse-EVA matrix composites was evaluated and compared with the behaviour of bagasse filled polypropylene (PP) and polyethylene (PE) matrix composites and wood-based materials. The volume fraction and size of the chopped bagasse used as filler were varied. The experimental results showed that the incorporation of bagasse strongly reduces the deformation capacity of the EVA copolymer. The impact strength was independent of the bagasse size, but varied with the volume fraction. As a function of the volume fraction it was shown that the mechanical performance of bagasse-EVA composites could be tailored to reproduce the behaviour of wood-base particleboards [88].

1.9 Objective of this study

The objective of this study was to prepare composites of an EVA copolymer with sisal fibre, and to investigate the effects of the fibre content and crosslinking on the physical properties of the composites, and to try and explain the results observed in terms of morphological changes and structural properties of EVA, sisal fibre and their composites.

CHAPTER 2

EXPERIMENTAL

2.1 Materials

2.1.1 Ethylene vinyl acetate co-polymer (EVA)

EVA 750 with 9 % vinyl acetate (VA) content, a density of 0.930 g cm^{-3}, melting point of 95 °C, tensile strength of 19 MPa and 750 % elongation at break, was supplied by Plastamid, Elsies River, South Africa.

2.1.2 Dicumyl peroxide (DCP)

DCP, supplied by Sigma-Aldrich, Johannesburg, South Africa, was used as cross-linking agent. It has a melting point of 39-41 °C [48], and decomposes at temperatures above 88 °C.

2.1.3 Sisal fibre

Sisal (*Agave sisalana*) fibre was obtained from the National Sisal Marketing Company in Pietermaritzburg, South Africa. These were supplied as very strong, cream-white fibres. The physical and mechanical properties of the sisal fibre are given in Table 2.1.

Table 2.1 Properties of sisal fibre

d/μm	σ/MPa	E/MPa	ε_b/%
100-300	490	11350	5

d = fibre diameterE = tensile modulus σ = ultimate strength ε_b = elongation at break

2.2 Methods

2.2.1 Preparation of composites

The long fibres were cut into small pieces with lengths between 5 and 10 mm. This fibre was washed with petroleum ether by soaking at 40 °C for 5 hours (regular shaking was necessary). It was then washed thoroughly with warm distilled water and dried at 80 °C overnight. 35 g samples of EVA, sisal fibre and DCP (where cross-linking was required) were mixed in different ratios and added simultaneously in a 55 cm^3 mixer of a Brabender Plastograph (Table 2.2). Mixing was done for 10 min. at a temperature of 120 °C and a mixing speed of 30 min^{-1}. The samples were then melt-pressed at 120 °C and 100 bar for 5 minutes.

Table 2.2 Composition of composite samples

w/w EVA/Sisal/DCP	w/w EVA/Sisal/DCP	w/w EVA/Sisal/DCP	w/w EVA/Sisal/DCP
100/0/0	100/0/01	100/0/02	100/0/03
90/10/0	90/10/01	90/10/02	90/10/03
80/20/0	80/20/01	80/20/02	80/20/03
60/40/0	60/40/01	60/40/02	60/40/03

2.2.2 Extraction

The gel content was determined through toluene extraction of the uncross-linked part of the samples. Samples were wrapped in fine stainless steel mesh and tied with a string, placed in a round-bottomed flask half-filled with toluene, and refluxed for 12 hours. After extraction, the wrapped samples were washed with chloroform and first dried at room temperature for 24 hours, followed by 50 °C drying in an oven for 24 hours, to evaporate all the chloroform. The samples were re-weighed and the gel content relative to EVA content was determined by calculating the percentage ratio of the mass of toluene-insoluble gel to that of the sample before extraction, using Equation 2.1.

$$\% \text{ gel} = (m_3 - (m_2 - xm_1) / xm_1) \times 100 \qquad (2.1)$$

where m_1 is the mass of sample before extraction, m_2 the mass of sample + mesh + copper wire before extraction, and m_3 is the mass of sample + mesh + copper wire after extraction and drying. x is the mass fraction of EVA in the original sample.

2.2.3 Differential scanning calorimetry (DSC)

DSC analyses were carried out on a Perkin-Elmer DSC 7 thermal analyser under nitrogen flow. The instrument was calibrated using the onset temperatures of melting of indium and zinc standards, and the melting enthalpy of indium. Polymer samples (between 5 and 10 mg) were initially heated from 25 to 150 °C at 10 °C min^{-1}, held at that temperature for one minute to eliminate thermal history effects, and then cooled to 25 °C at 10 °C min^{-1}. They were maintained there for one minute, heated again up to 150 °C at 10 °C min^{-1}, and cooled to 25 °C at the same rate. Onset and peak temperatures of melting and crystallization, as well as melting and crystallization enthalpies, were determined from the second scan where ΔHm is the melting enthalpy of the samples calculated from the main melting peak.

2.2.4 Thermogravimetric analysis (TGA)

Thermogravimetric analyses were carried out on a Perkin-Elmer TGA 7 thermogravimetric analyzer. Polymer samples (between 5 and 10 mg) were heated from 25 to 600 °C at 20 °C min^{-1} under flowing nitrogen.

2.2.5 Surface energy evaluation

For the determination of the total surface energy, as well as its disperse and polar parts, a surface energy evaluation system (SEES, Czech Republic) was used. Contact angle measurements were done by the drop method using the Owens-Wendt regression method. Five liquids of different polarity were used (water, aniline, formamide, benzyl alcohol and ethylene glycol). Each measurement was repeated 15 times to ensure reproducibility.

2.2.6 Tensile testing

The mechanical properties were determined using a Hounsfield H5KS tensile tester at a cross-head speed of 50 mm min^{-1}. Dumbbell shaped specimens with a thickness of 1.3 mm,

average width of 4.9 mm and gauge length of approximately 24 mm were used. In total, five dumbbells per composite sample were used for each analysis and the average was taken as the reported value.

2.2.7 Scanning electron microscopy

The morphological aspects of the sisal-EVA interfaces at fracture surfaces were observed by using a Jeol 6400 WINSEM scanning electron microscope at 5 keV.

2.2.8 Porosity

A mercury porosimetry method was used for the determination of the total volume between the EVA monofilaments, the pore volumes in the EVA composite with treated and untreated fibres, the evaluation of pore size distributions, as well as the determination of the specific surface. The measurements were carried out in a Porozimetro 1500 Carlo Erba instrument connected to a calculation unit CVT 960. The maximum pressure of mercury used was 150 MPa, which allowed determination of pore sizes down to 5 nm.

2.2.9 Fourier transform infrared spectroscopy (FTIR)

Analyses were done in a Shimadzu FTIR 8700 spectrometer combined with a highly sensitive MCT detector connected to an infrared microscope AIM 8800. Spectra were recorded from 720 to 4000 cm^{-1} at a 4 cm^{-1} resolution. An ATR objective with a germanium crystal (magnification 15x) was used. The detected area was 100 x 100 μm.

CHAPTER 3

RESULTS AND DISCUSSION

3.1 Characterization of materials and composites

3.1.1 Gel content

Table 3.1 Gel content (in wt %) of EVA-sisal composites prepared in the absence and presence of DCP

EVA-sisal	0 % DCP	1 % DCP	2 % DCP	3 % DCP
100 / 0	0.0	3.1	3.2	10.3
90 / 10	5.1	10.5	16.3	19.2
80 / 20	7.1	17.6	23.9	27.4
60 / 40	7.8	30.4	48.3	50.1

Table 3.1 gives a summary of the gel content in both the untreated and DCP treated EVA-sisal composites. The dependence of the gel content on the sisal content in the composites for various DCP concentrations is shown in Figure 3.1. The pure EVA samples processed in the presence of DCP only show a small increase in gel content. This increase is the result of cross-linking under the reaction conditions. The cross-linking is, however, much less pronounced than expected. The most probable reason is that mixing took place at 120 °C for 10 minutes, which is not long enough for a sufficient amount of DCP to decompose in order to initiate substantial cross-linking (the half-life of DCP at 120 °C is 420 minutes). Introducing fibre in the matrix in the absence of DCP gives rise to a slight increase in gel content. Thermomechanical friction in the Brabender mixer probably causes grafting between the sisal fibre and the EVA matrix, even in the absence of peroxide. The increase in temperature as a result of the friction probably provided enough energy to initiate a reaction between the active groups on EVA and sisal respectively, giving rise to grafting. In the presence of DCP there is an increase in gel content with increasing sisal fibre content. This increase is more substantial at higher DCP contents. During mixing the programmed temperature was 120 °C, but due to the friction in the presence of a high fibre content, it

increased to 127 °C. This could lead to more efficient cross-linking of EVA, but all indications are that grafting between EVA and sisal fibre took place, especially at high fibre and DCP contents (see discussion later on).

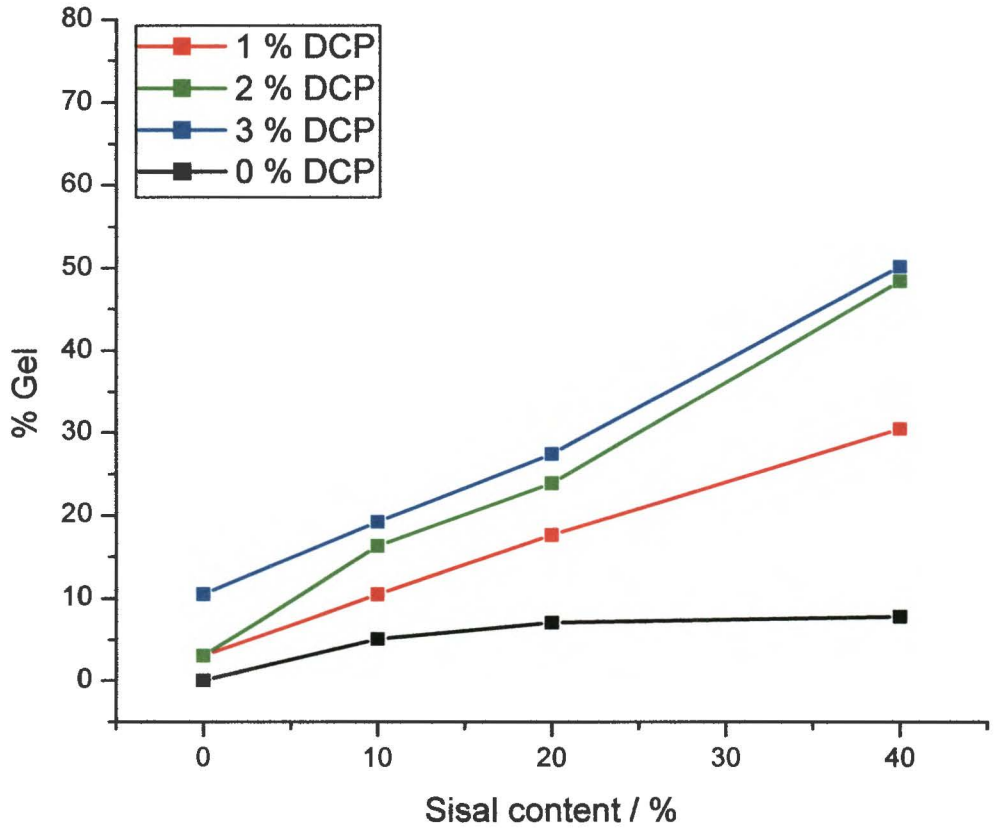

Figure 3.1 Gel content of EVA/sisal composites prepared in the absence and presence of DCP

3.1.2 Fourier-transform infrared spectroscopy (FTIR)

For a possible confirmation of grafting, infrared spectra were obtained. A highly magnified cross-section of EVA-sisal fibre (prepared in the presence of 3 wt.% DCP) was analysed by FTIR. As Figure 3.2 shows, eight different areas were scanned by the FTIR spectrometer, and the spectra are shown in Figure 3.3 (spectrum A is missing, because it is the same as spectrum H). For a more thorough investigation of the EVA-sisal fibre interface,

spectra were obtained for the interface, pure EVA and pure sisal fibre (Figure 3.4). The spectrum of the pure EVA matrix consists of strong C-H vibrations in the 2850 and 2920 cm^{-1} regions. The peak belonging to the acetyl group (vibration of the C=O ester of the carboxyl group) appears at 1730 cm^{-1}. In the case of sisal fibre, a huge broad peak appears at 3360 cm^{-1} that belongs to the OH group. Provided that chemical bonding (grafting) was observed, a decrease in acetyl groups (EVA – Figure 3.5) and a simultaneous decrease in OH groups (sisal fibre) should be observed at the interface. Grafting between EVA and sisal fibre will be the result of a reaction between these two groups. Confirmation of this is shown in Figure 3.4 (fibre-matrix interface), where a strong decrease in peak intensity is observed for the peaks at 1730 and 3360 cm^{-1}.

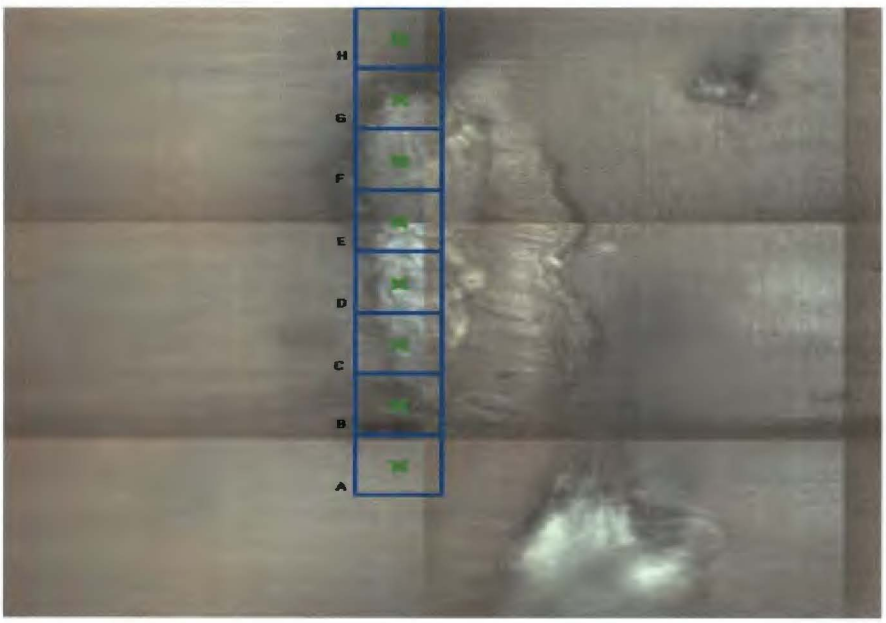

Figure 3.2 Cross-sectional areas of the EVA-sisal interface analysed by FTIR

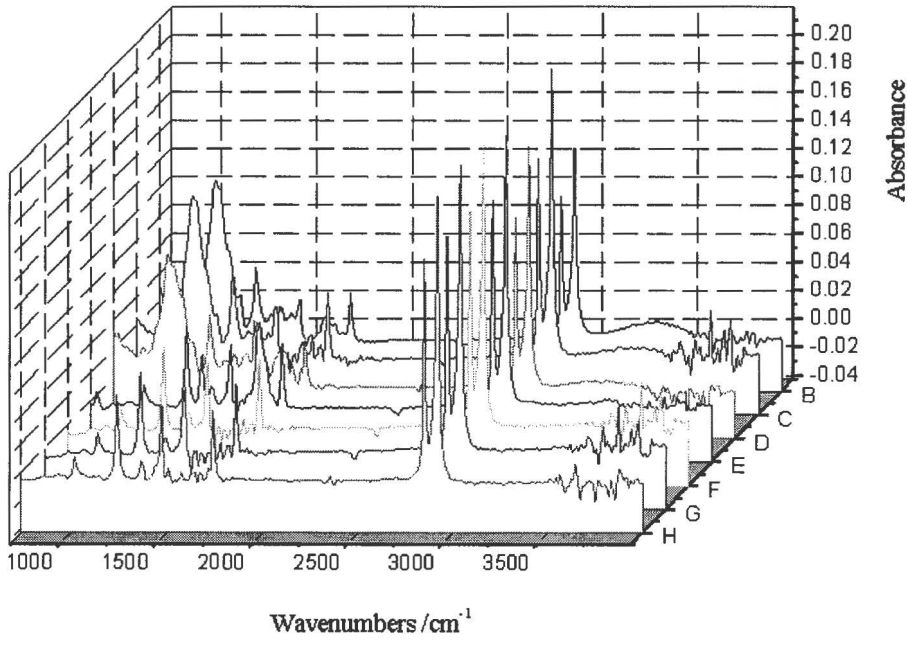

Figure 3.3 FTIR spectra of the different point marked on Figure 3.2

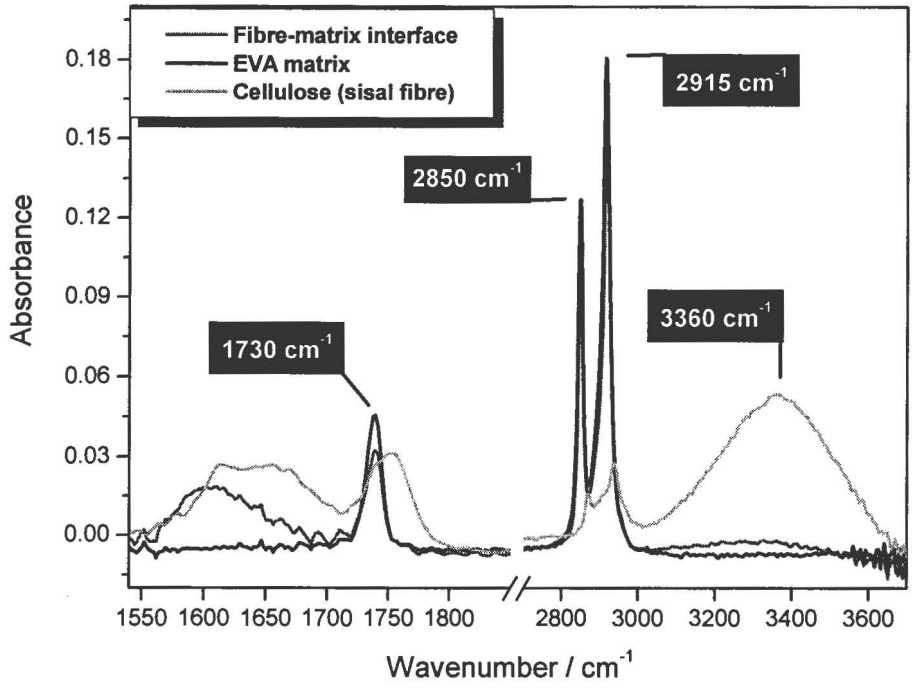

Figure 3.4 FTIR spectra of EVA, sisal fibre and the EVA-sisal interface in a 3 % DCP composite

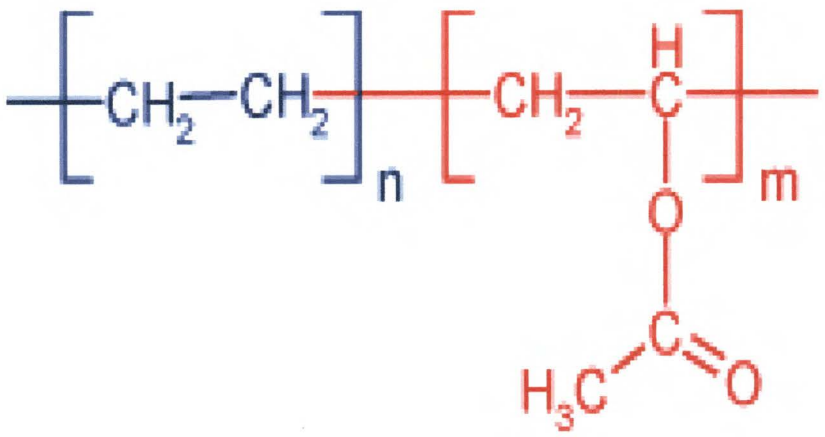

Figure 3.5 Structure of the EVA co-polymer

A possible mechanism for the grafting between EVA and sisal fibre initiated by DCP is shown in Figure 3.6. Initially the peroxide generates primary radicals upon thermal decomposition at an elevated temperature. These primary radicals abstract hydrogen from the sisal CH_2OH groups to form –C• radicals, and from carbons on the backbone chain linked to the acrylate groups to form –C• radicals. These two radicals combine to form a grafting link.

3.1.3 Scanning electron microscopy (SEM)

SEM micrographs of the fracture surface of untreated and 3 % DCP treated EVA-sisal composites (40 % fibre loading) are shown in Figure 3.7 and 3.8 respectively. It can be seen that in the untreated composites the fibres are pulled out from the matrix, creating vacant spaces (canals) during fracture (see arrow in Figure 3.7), while in the samples treated with 3 % DCP, the fibres undergo de-lamination, and there is no indication of the fibres being pulled from the matrix. This clearly indicates grafting between EVA and sisal fibre, as already shown by the FTIR results discussed above.

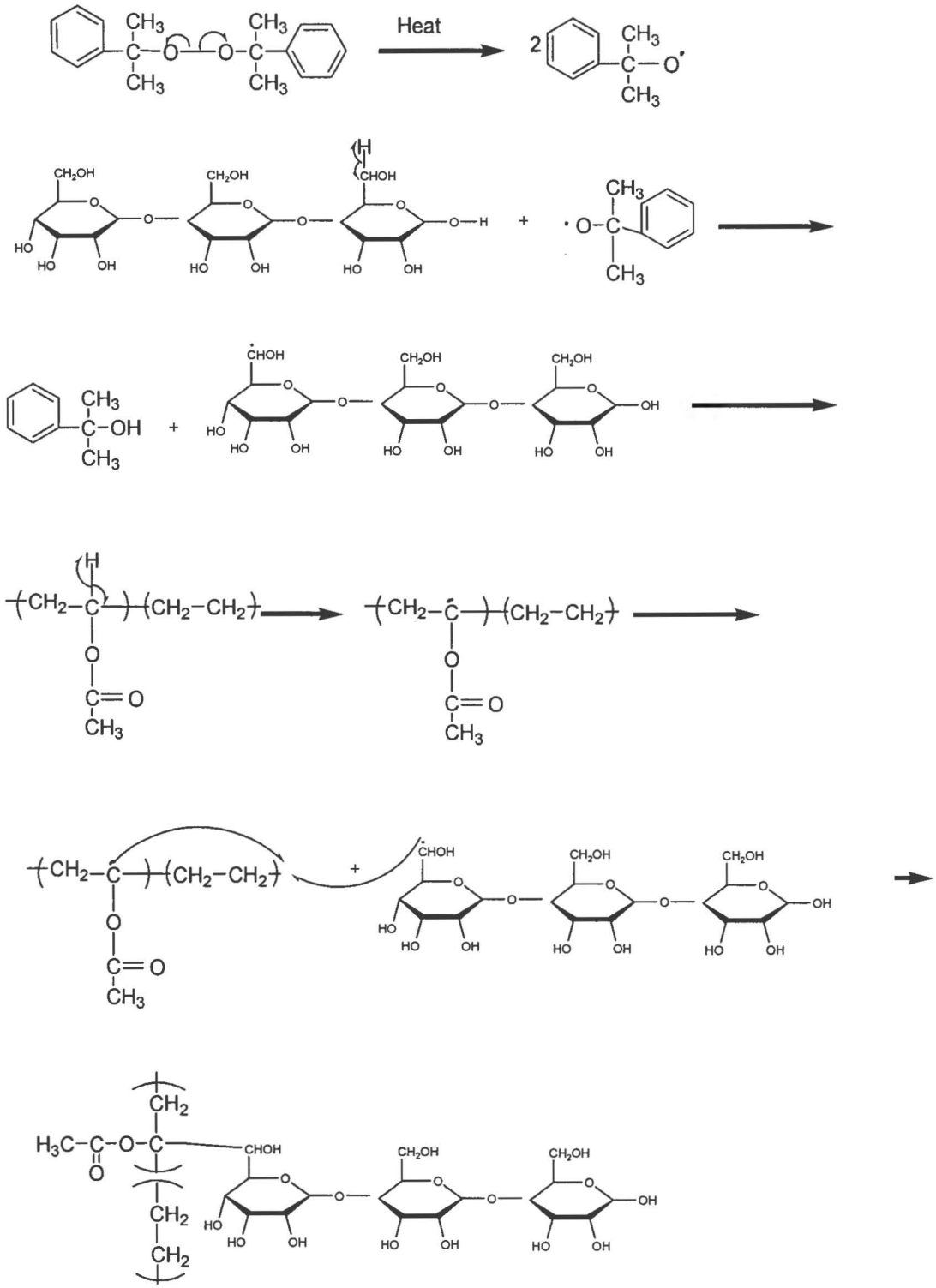

Figure 3.6 Possible mechanism for EVA-sisal grafting in the presence of DCP

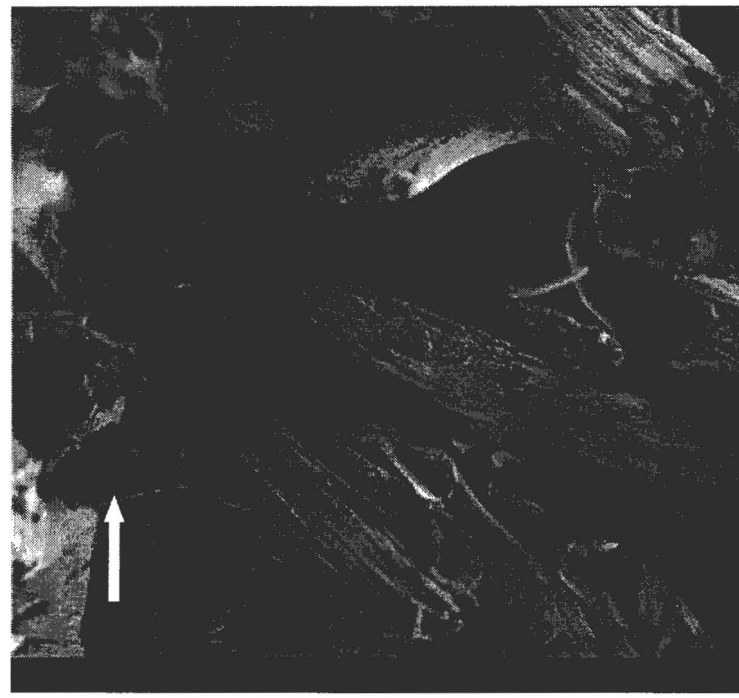

Figure 3.7 **SEM micrograph of the fracture surface of an untreated EVA-sisal composite (40 % of fibre loading)**

Figure 3.8 **SEM micrograph of the fracture surface of a treated EVA-sisal composite (40 % of fibre loading and 3% DCP)**

3.1.4 Porosity

Despite the fact that sisal fibre looks like a monofilament, it is clear from the Hg-porosimetry of sisal fibres (solid line, Figure 3.9) and from the SEM micrograph that sisal fibre is not a monofilament, but a multifilament (the mark of sisal on the EVA matrix). Another confirmation of this is the size of pores being higher than 20 μm (> log r_p = 4). We can assume that these pores come from the inter-filament areas. The volume ratio of these pores is approximately 20 %. From the Hg-porosimetry of sisal fibres is also evident that there are two different types of pores. The first peak appears at a log r_p of approximately 2.5, which is equivalent to 700 nm (diameter of pores). The volume of these pores is 0.160 $cm^3.g^{-1}$. The second peak appears at approximately log r_p = 1.75 which is equivalent to 110 nm. The volume of these pores is 0.339 $cm^3.g^{-1}$. From this it is evident that the very small pores of approximately 100 nm make up the largest part of the pore volume in the sisal fibre. In the EVA-sisal fibre sample the volume ratio of the pores, with log r_p higher than 4, decreased from 20 % to 9 %. There is also a substantial decrease in the sizes of the other two peaks (in the case of log r_p = 2.5 the decrease is from 0.160 to 0.035 $cm^3.g^{-1}$, and in the case of log r_p = 1.75 the decrease is from 0.339 to 0.155 $cm^3.g^{-1}$). From this it is evident that the pure EVA matrix has a substantial effect on the filling of the pores in the sisal fibre. This, of course, depends on the viscosity of the blend during the mixing in the Brabender. This effect is even more pronounced for the sample prepared in the presence of 3 %. Compared to the EVA/sisal fibre composite, the volume of the pores with log r_p higher than 4 and log r_p = 2.5 decreased to the same level as that of the pure EVA matrix. In the case of log r_p = 1.75 the decrease is from 0.339 $cm^3.g^{-1}$ (for the sisal fibre) and from 0.155 $cm^3.g^{-1}$ (for the EVA/sisal composite) to 0.047 $cm^3.g^{-1}$. This substantial decrease in the pore volume, especially when the sample is prepared in the presence of DCP, can be explained as follows: GPC analysis did not show a decrease in molecular weight of the EVA matrix prepared in the presence of DCP, which means that degradation and the accompanying decrease in viscosity is negligible. This can therefore not be the reason for the decrease in pore volume observed for the composite sample prepared in the presence of DCP. From the gel content results it is evident that there should be a slight increase in viscosity, because cross-linking of EVA in presence of DCP was measured. This increase is negligible, because the torque detected by the probe immersed in the Brabender mixer does not show a substantial increase in torque. The only logical explanation for such a big decrease in pore volume is that grafting between the EVA chains

and the sisal fibre took place. The molecules of Hg cannot easily fill the pores in the sisal structure, because chemical bonding with the EVA matrix is probably already present.

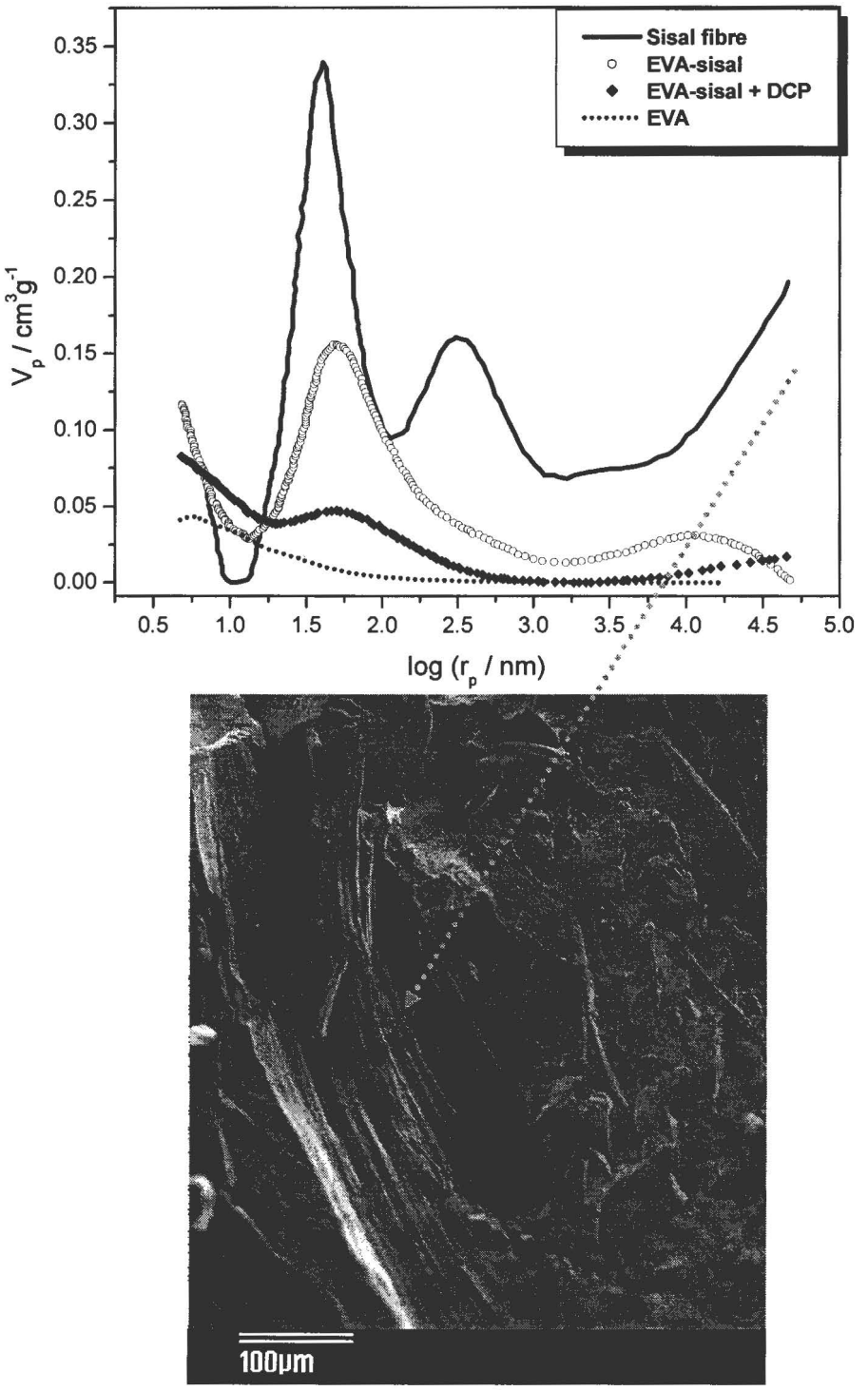

Figure 3.9 **Hg-porosimetry curves of sisal fibre, EVA, EVA-sisal composite, and EVA-sisal-DCP linked to an SEM micrograph of the EVA-sisal composite**

3.2 Properties of the composites

3.2.1 Thermal properties

3.2.1.1 Differential scanning calorimetry (DSC)

The DSC curves are shown in Figures 3.10 – 3.17, and they all show only one melting or crystallization peak. The onset and peak temperatures, as well as experimentally observed and theoretically expected (taking into account EVA/sisal ratios and assuming EVA has the same melting behaviour than in the absence of sisal) enthalpies are summarised in Table 3.2.

Table 3.2 Summary of DSC melting data for DCP treated and untreated EVA-sisal composites

EVA-sisal-DCP	$T_{p,m}$ / °C	$T_{o,m}$ / °C	Experimental ΔH_m / J g^{-1}	Expected ΔH_m / J g^{-1}
100-0-0	97.4	87.3	56.7	
90-10-0	97.1	86.2	41.6	51.1
80-20-0	95.2	86.5	36.2	45.4
60-40-0	94.4	84.7	27.2	34.1
100-0-1	96.7	89.5	42.3	
90-10-1	96.2	87.1	39.1	38.1
80-20-1	96.1	86.2	36.3	33.8
60-40-1	96.2	81.9	24.4	25.4
100-0-2	96.6	87.9	41.8	
90-10-2	96.2	86.9	38.1	38.2
80-20-2	95.8	86.6	33.5	33.8
60-40-2	95.4	82.1	23.3	24.7
100-0-3	95.2	84.8	37.2	
90-10-3	95.1	84.4	33.1	33.5
80-20-3	95.2	84.4	27.6	29.8
60-40-3	94.9	81.4	20.8	22.3

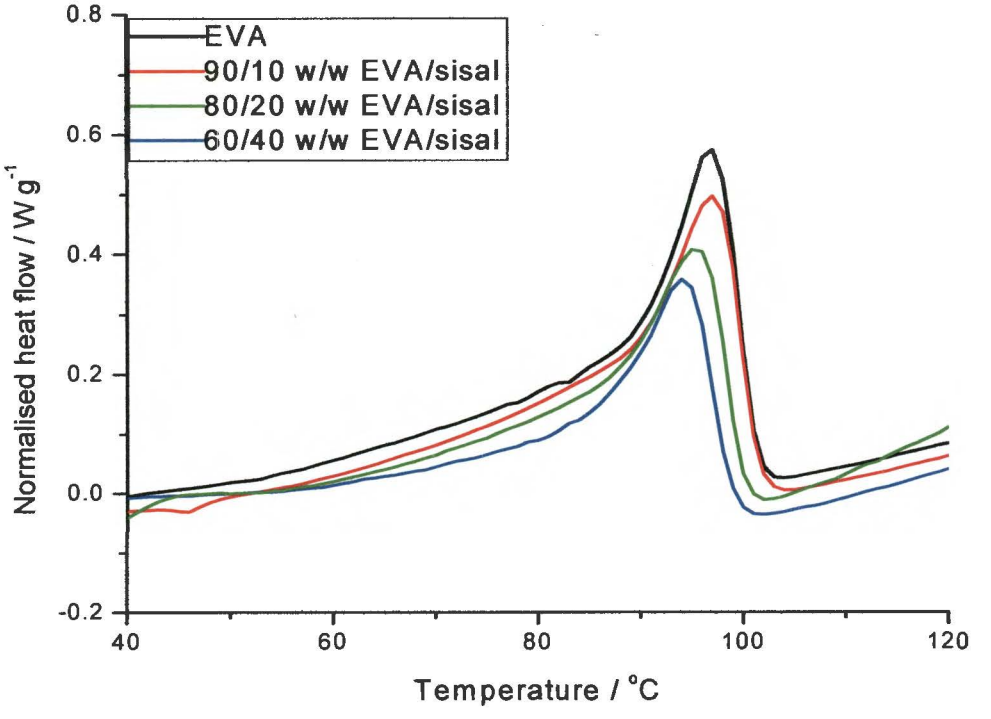

Figure 3.10 DSC heating curves of pure EVA and untreated EVA-sisal composites

The DSC heating curves of the untreated composites in Figure 3.10 show single endothermic peaks between 80 and 100 °C, which are the EVA melting peaks. As expected, the size of the peak decreases with increasing sisal content, because only the EVA part of the composite melts. The experimental enthalpy of 56.7 J g^{-1} of pure EVA decreases to 41.6 J g^{-1} in the presence of 10 % sisal, to 36.2 J g^{-1} in the presence of 20 % sisal, and to 27.2 J g^{-1} in the presence of 40 % sisal. Assuming there was no change in crystallization behaviour in the presence of sisal, the enthalpies of the composites should have been 51.1, 45.4 and 34.1 J g^{-1}, respectively. This suggests that sisal fibre hinders the crystallization of the EVA chains. At a sufficiently high temperature, the EVA part in the composites forms an amorphous melt in which the chains are entangled in random coils undergoing thermal motion. Because of the polar nature of both substances, there probably is an attraction between them which influences the crystallization behaviour of EVA. Increasing sisal content also causes the EVA to melt at lower temperatures, indicating a decrease in lamellar thickness in addition to the decreasing crystallinity.

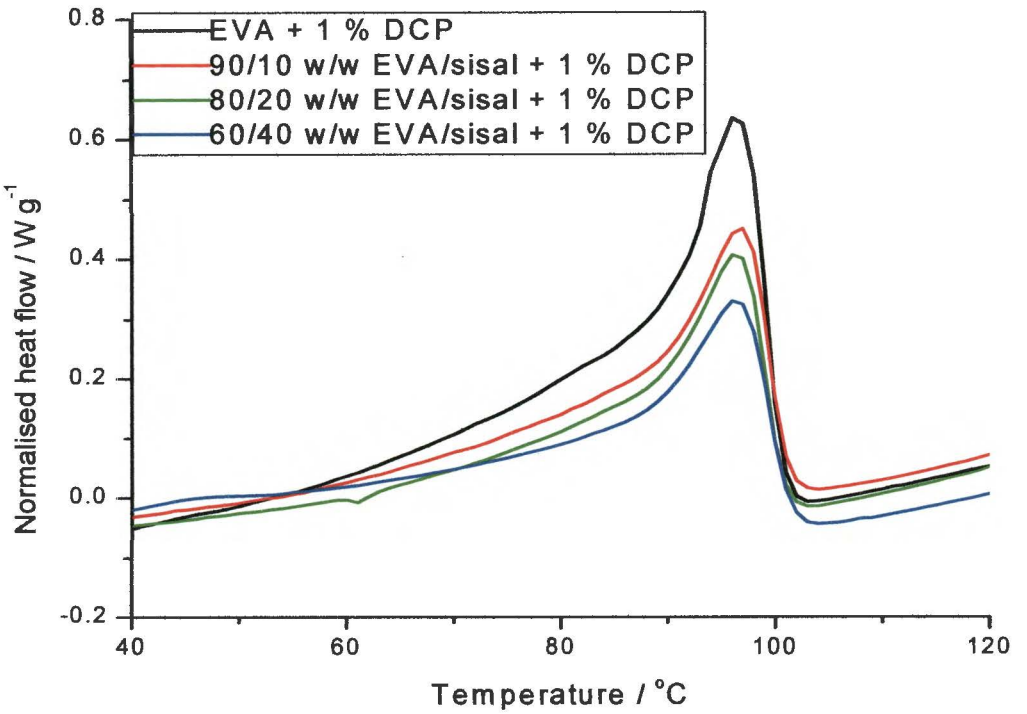

Figure 3.11 DSC heating curves of 1 % DCP treated EVA and EVA-sisal composites

The spatial arrangement of the crystalline and amorphous phase controls the physical properties of a solid polymer, especially at larger strains and during fracture. The way crystalline lamellae are formed in the process of crystallization by folding the chains yields a considerable amorphous fraction on the surface of crystallites and within the interlamellar space. Figure 3.11 shows the DSC curves of composites prepared in the presence of 1 % DCP. The melting temperatures of the composites are almost the same as that of EVA with 1 % DCP, which indicates that in the presence of slight cross-linking/grafting the lamellar thickness does not decrease. There is also a good correlation between the expected and experimental enthalpies, indicating that the crystallinity did not change for these samples.

Figure 3.12 shows a very slight decrease in peak temperature of melting of the 2 % DCP treated samples. The experimentally observed enthalpies are again in line with the expected enthalpies. This again seems to point to very little change in lamellar thickness and total crystallinity for composites prepared in the presence of DCP.

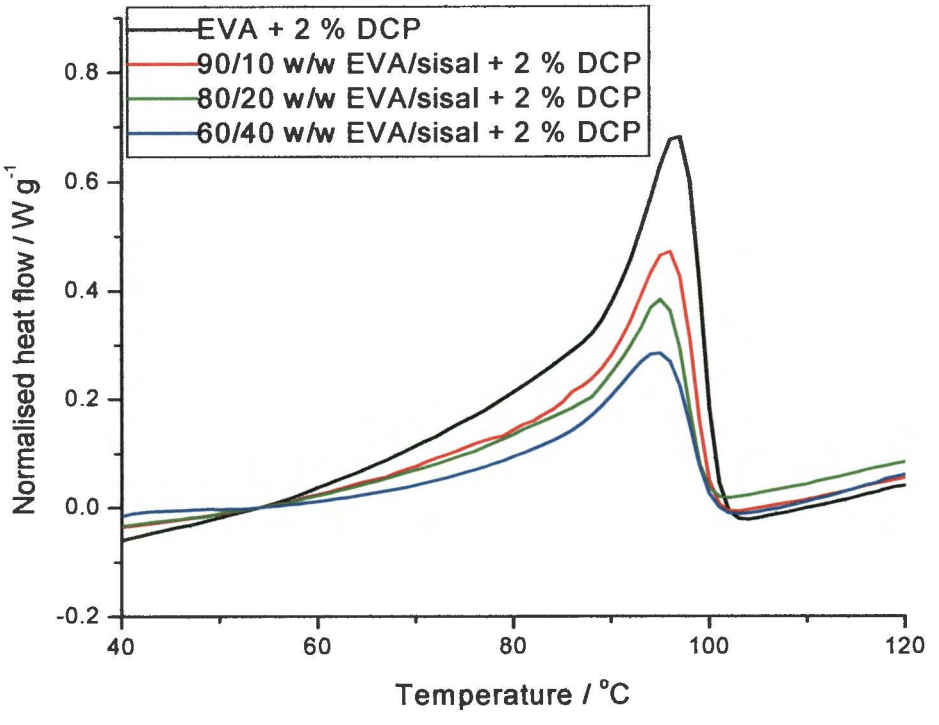

Figure 3.12 DSC heating curves of 2 % DCP treated EVA and EVA-sisal composites

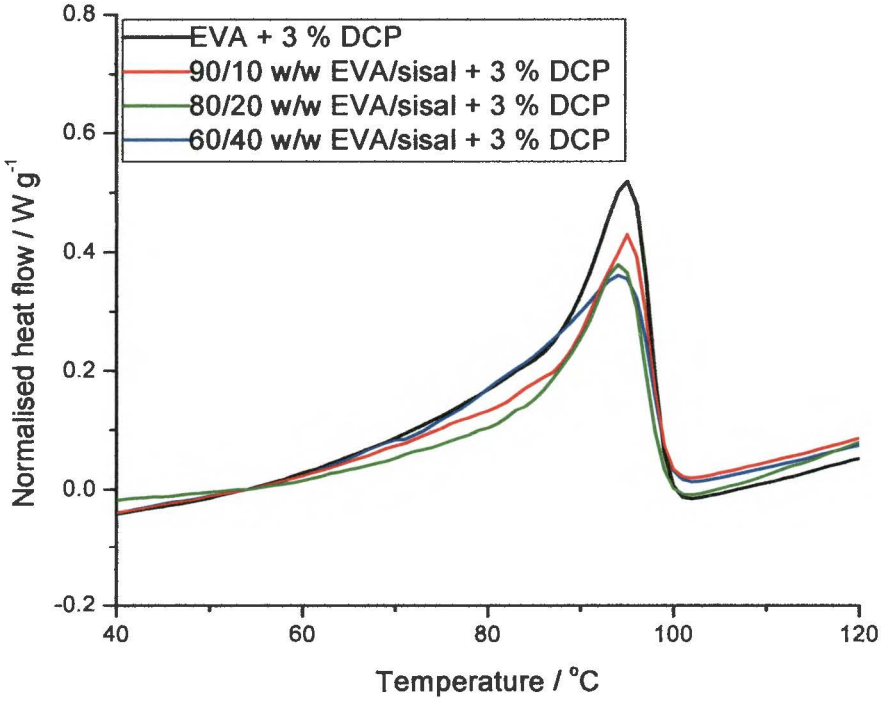

Figure 3.13 DSC heating curves of 3 % DCP treated EVA and EVA-sisal composites

The DSC melting curves for 3 % DCP treated EVA-sisal composites are plotted in Figure 3.13. As is the case of the samples prepared in the presence of 1 and 2 % DCP, the peak temperatures were not influenced by the presence of increasing amounts of sisal. The melting enthalpies are, however, lower than the expected enthalpies for the samples containing 20 and 40 % sisal. Although the lamellar thickness did not seem to change, there was a slight decrease in total crystallinity. This is probably due to grafting which restricts chain folding, and which results in epitaxial crystallization of EVA chains on the surfaces of the sisal fibres, giving rise to lower crystallinity.

From the FTIR results and the possible mechanism of grafting, it can be assumed that as the number of active sites on a polymer chain increases, cross-linking will start taking place in addition to grafting. As the chains become more connected in three dimensions, the entire sample becomes one large molecule. This will inhibit crystallization and influence the degree of crystallinity.

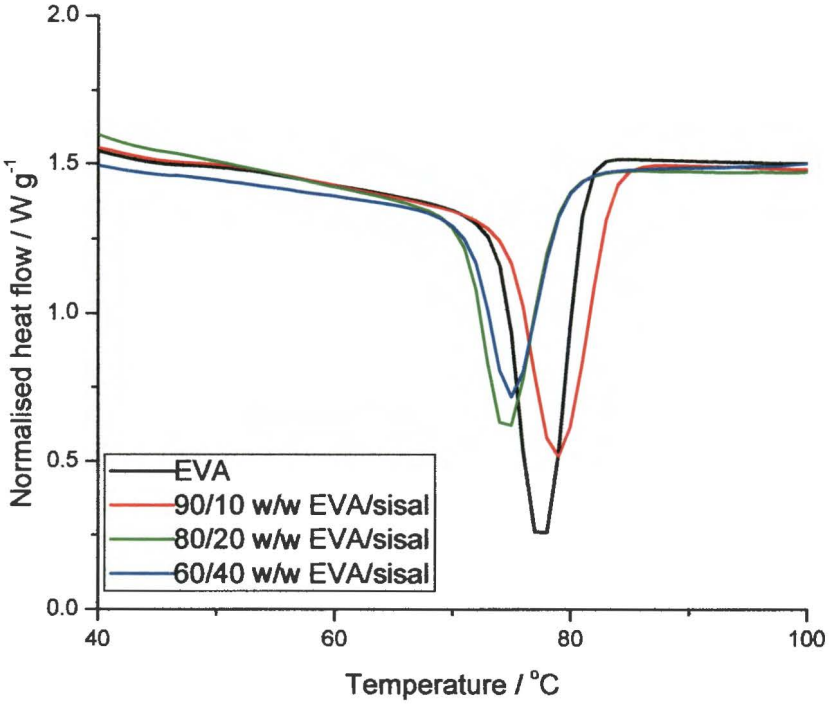

Figure 3.14 DSC cooling curves of untreated EVA and EVA-sisal composites

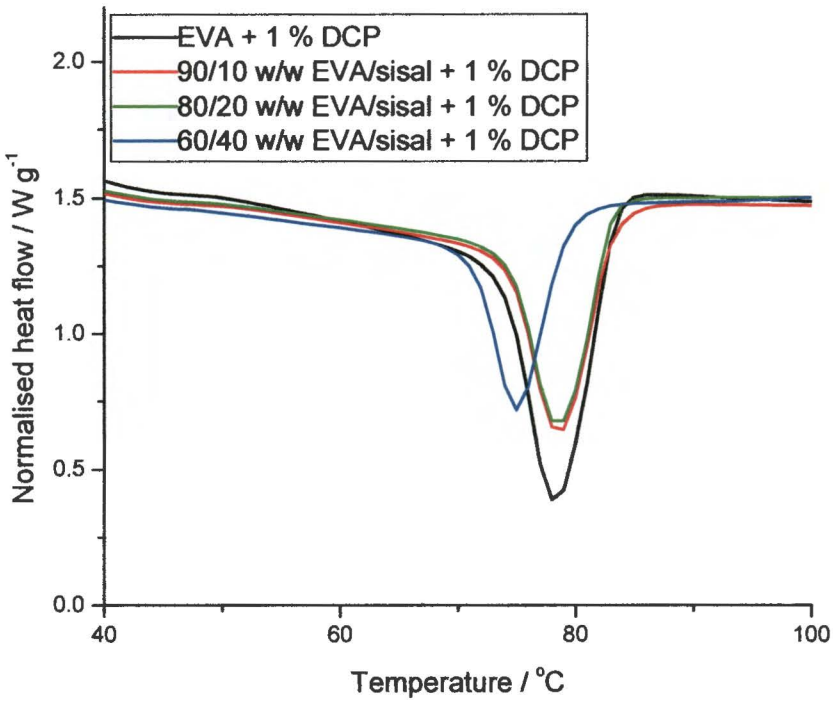

Figure 3.15 DSC cooling curves of 1 % DCP treated EVA and EVA-sisal composites

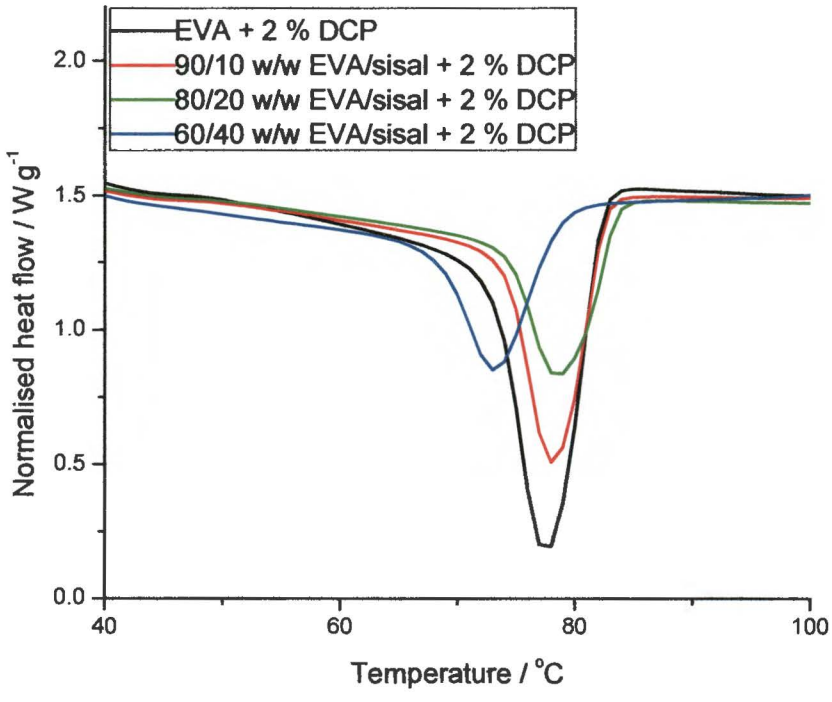

Figure 3.16 DSC cooling curves of 2 % DCP treated EVA and EVA-sisal composites

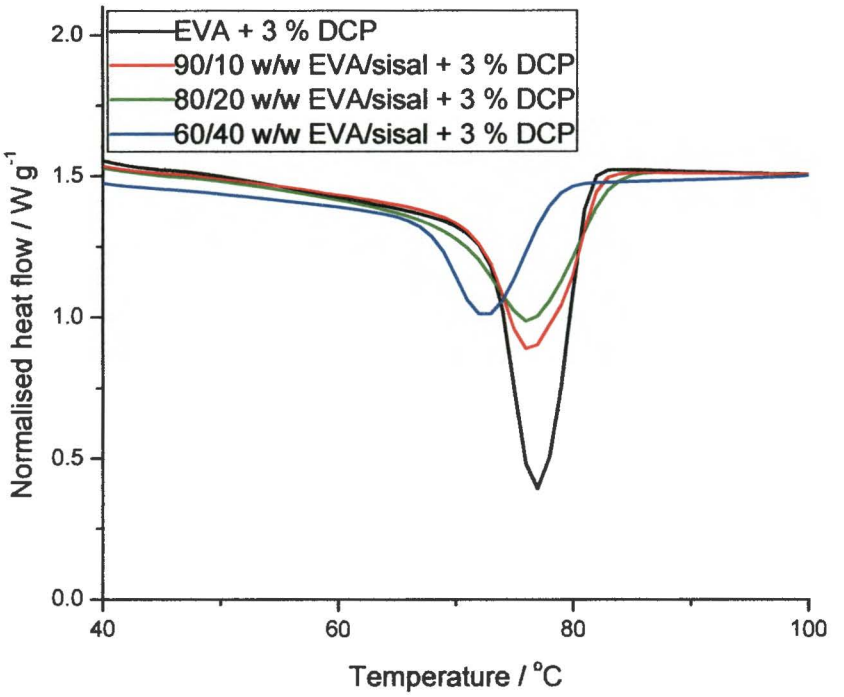

Figure 3.17 DSC cooling curves of 3 % DCP treated EVA and EVA-sisal composites

The DSC cooling curves of the composites are shown in Figures 3.14 - 3.17. In the case of the untreated EVA and EVA-sisal composites (Figure 3.14) the EVA starts crystallizing at a higher temperature in the case of the 90/10 w/w EVA-sisal composite, but at lower temperatures for the other two composites. This clearly indicates that sisal influences the crystallization behaviour of EVA. This is, however, not reflected in the re-heating results (see discussion above), indicating secondary crystallization effects during and after initial crystallization. The DCP treated samples show similar crystallization behaviour (Figures 3.15 – 3.17), although the differences are not so pronounced. This is probably due to cross-linking/grafting having an inhibition effect on the crystallization behaviour. In all three the last cases the 70/30 w/w EVA-sisal samples show a much lower crystallization temperature, indicating the formation of thinner lamellae. This is probably due to grafting which restricts chain folding, and which results in only epitaxial crystallization of EVA chains on the surfaces of the sisal fibres. This causes the formation of relatively thin lamellae, with the resultant decrease in crystallization temperature

3.2.1.2 Thermogravimetric analysis (TGA)

Figures 3.18 and 3.19 are respectively the TGA and DTGA curves of EVA, sisal fibre and the untreated composites. In the case of sisal fibre the mass loss between 60 and 100 °C corresponds to evaporation of water in the sample. The second mass loss, starting at about 300 °C, is due to the thermal depolymerization of hemicellulose and the cleavage of glucosidic linkages of cellulose. The third mass loss, starting at about 410 °C, may be due to the further breakage of the decomposition products of stage II leading to the formation of tar through levoglucosan. In the case of EVA two degradation steps are observed. The initial step involves the formation of acetic acid through decomposition of vinyl acetate, and the second one is the degradation of the main chains [52]. The composites show three mass loss steps. The first corresponds to the evaporation of water, and it seems as if the presence of EVA reduces water adsorption on the fibre. The second corresponds to the decomposition of sisal, and there is a direct correlation between the percentage mass loss in this step and the amount of sisal mixed into this sample. It is interesting that this decomposition occurs at substantially higher temperatures than that of pure sisal. The third corresponds to the decomposition of EVA, which also occurs at substantially higher temperatures than that of pure EVA. It seems as if both sisal and EVA are thermally more stable when combined into a composite, probably because of physical interaction and/or chemical grafting. The amounts of residue left at the end of the analyses indicate that only sisal decomposition products contribute to the formed residue, as discussed above.

For the DCP treated EVA in Figure 3.20 a small decrease in stability is observed with increase in DCP content. This suggests that there is some degradation in the presence of DCP, which becomes more pronounced with increasing DCP content. Figures 3.21 – 3.23 show the same small reduction in thermal stability with increase in DCP content. The size of the first step also increases in the presence of higher sisal contents, and corresponds with the amount of sisal initially mixed into the composite.

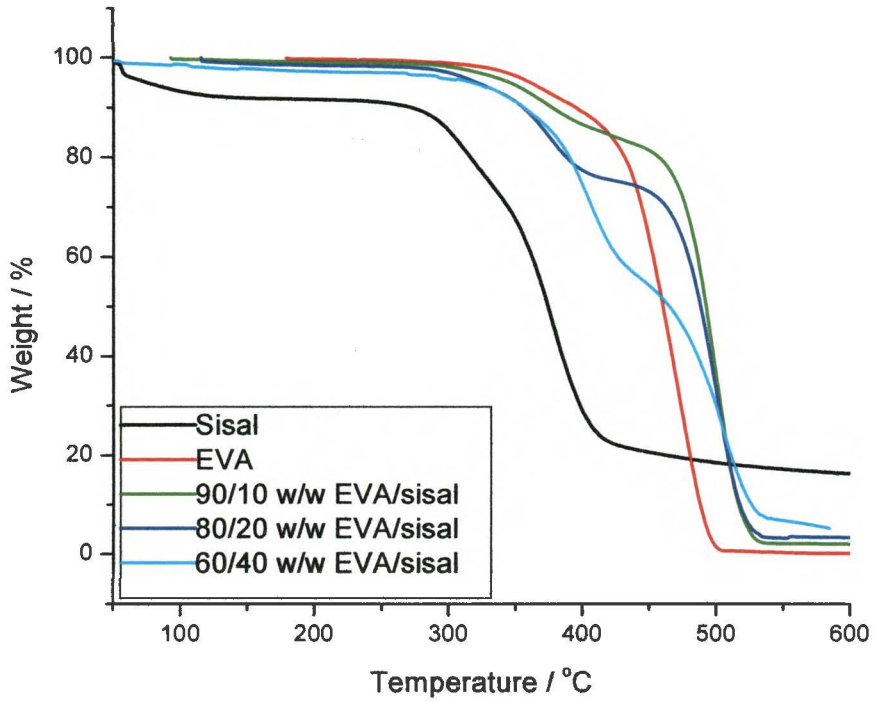

Figure 3.18 TGA curves of pure sisal, EVA and composites

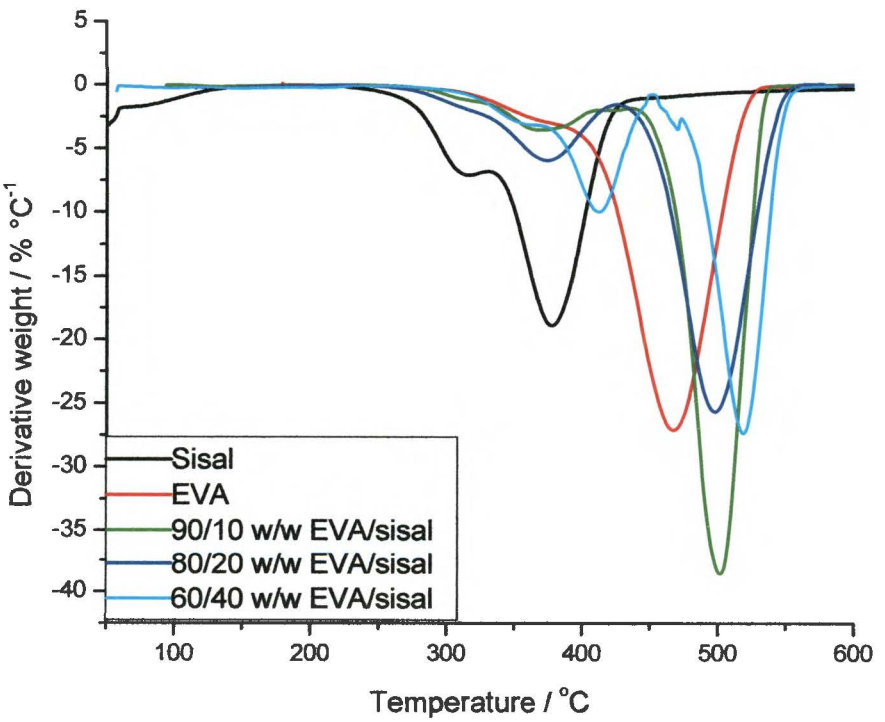

Figure 3.19 DTGA curves of pure sisal, EVA and composites

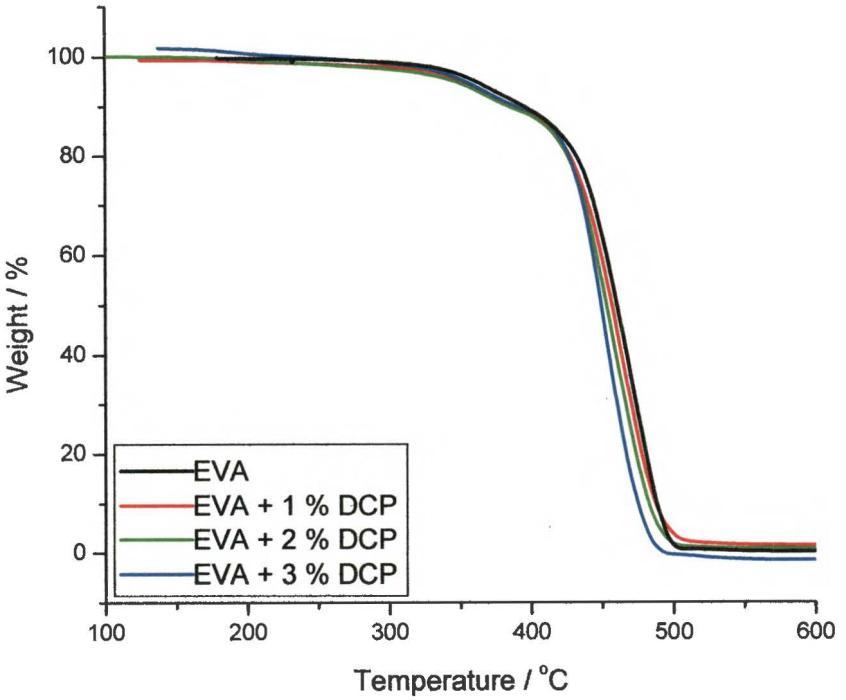

Figure 3.20 TGA curves of untreated and DCP treated EVA

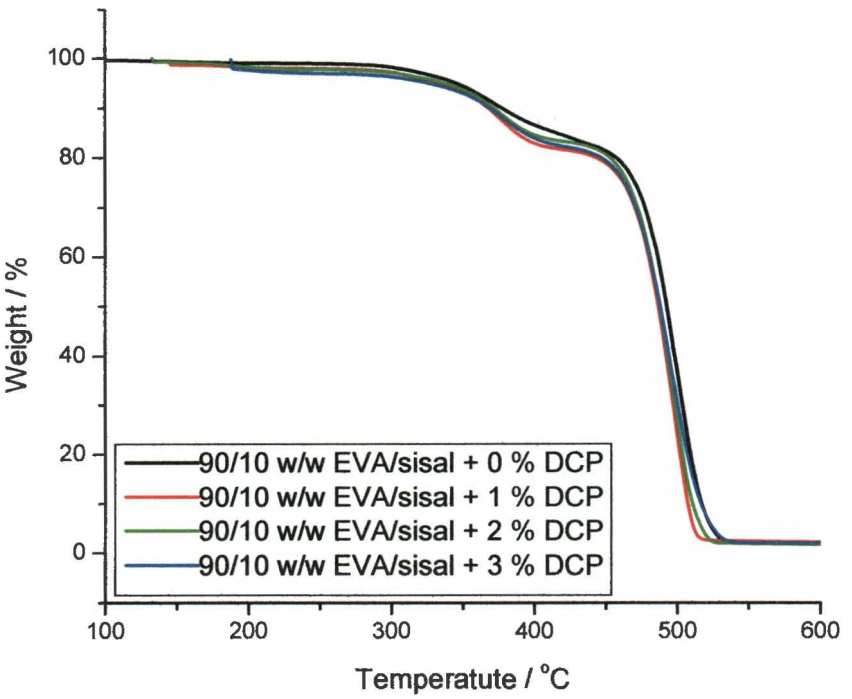

Figure 3.21 TGA curves of untreated and DCP treated 90/10 w/w EVA-sisal composites

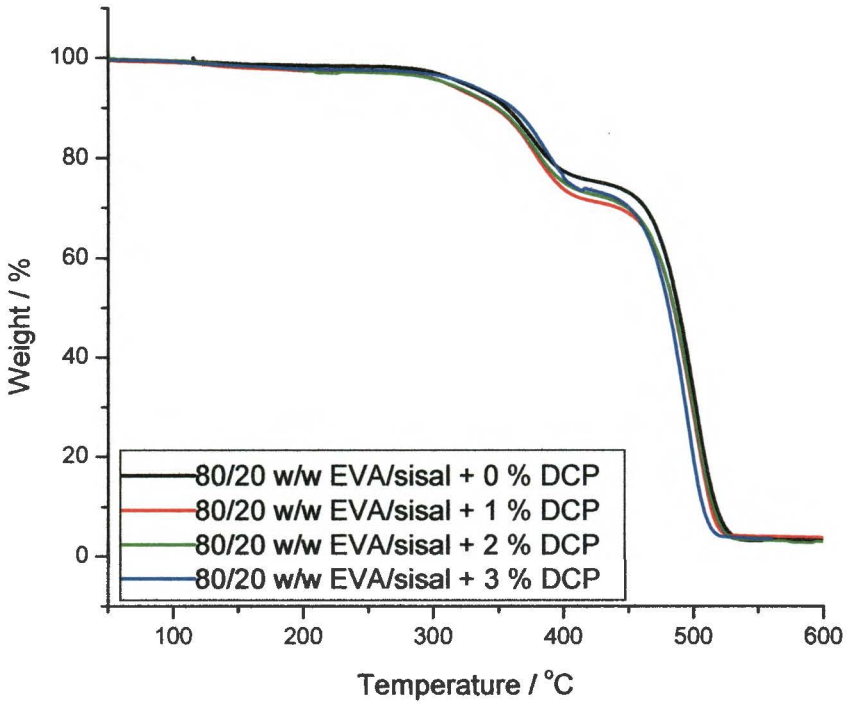

Figure 3.22 TGA curves of untreated and DCP treated 80/20 w/w EVA-sisal composites

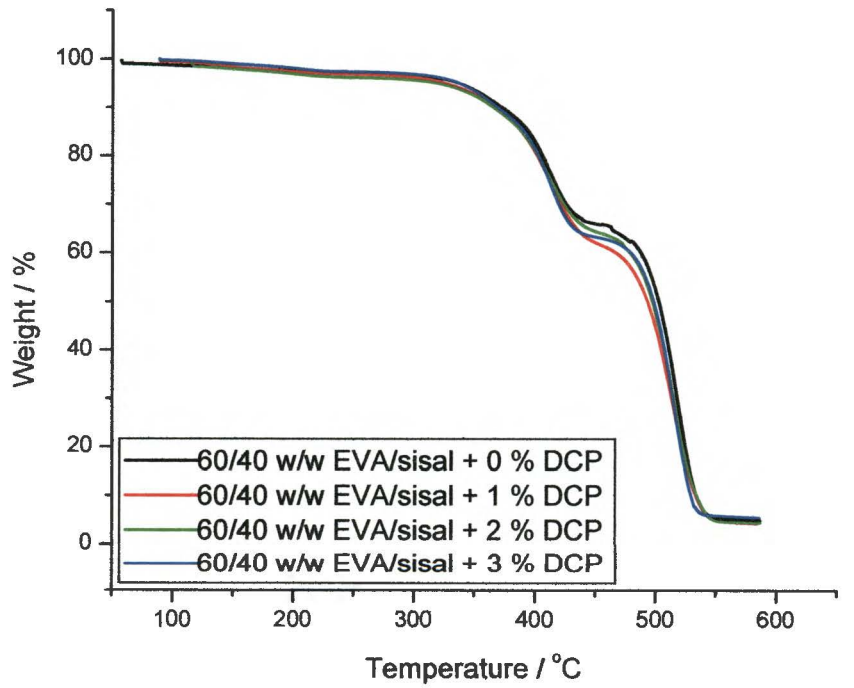

Figure 3.23 TGA curves of untreated and DCP treated 60/40 w/w EVA-sisal composites

3.2.2 Mechanical properties

The grafting and cross-linking have a substantial impact on the mechanical properties. The stress at break for EVA (in the absence of sisal) decreases with increasing DCP content (Figure 3.24, Table 3.3). Since cross-linking reduces crystallinity, this observation is expected. The presence of 10 wt.% sisal considerably reduces the stress at break of EVA, even for samples prepared in the presence of DCP. The reason is probably the weak interaction between EVA and sisal, and since it does not seem as if there is substantial grafting at this fibre load (Figure 3.1), a decrease in ultimate strength should be expected. Increased sisal contents give rise to increased stress at break values, especially for the samples prepared in the presence of increased amounts of DCP. Since it has been established that there is a strong element of grafting between EVA and sisal fibre (see discussion above), there will be stronger interaction between EVA and sisal fibre which should give rise to increasing stress at break values. Cross-linking and grafting restrain chain movement, giving rise to decreasing elongation at break (Figure 3.25, Table 3.3). Increasing sisal content as well as cross-linking and grafting give rise to higher values of Young's modulus and the elastic modulus at 5 % elongation (Figure 3.26 and 3.27 Table 3.3).

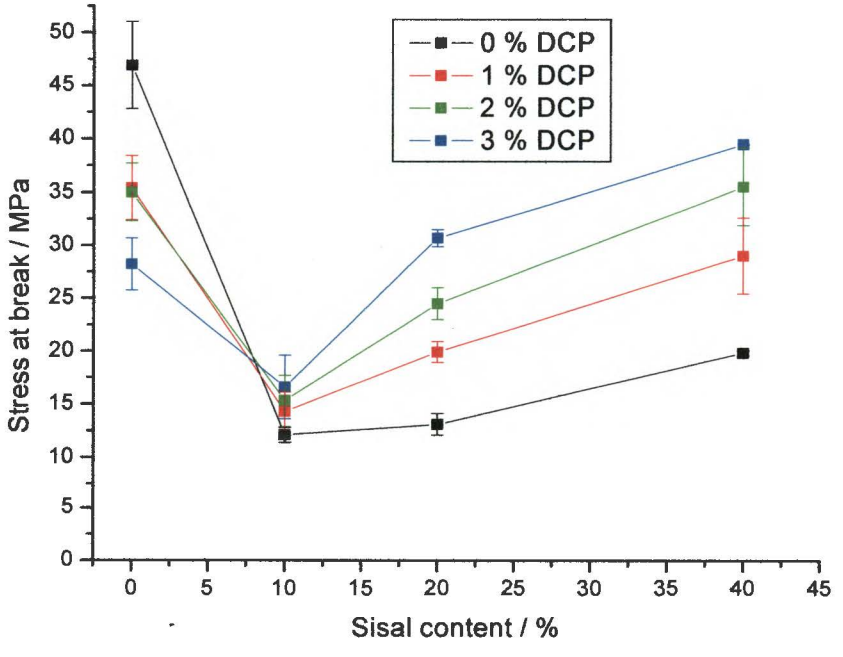

Figure 3.24 Effect of sisal content on the stress at break of the composites

Table 3.3 Mechanical properties of untreated and DCP treated EVA-sisal composites

EVA-sisal-DCP	$\varepsilon_b \pm s\varepsilon_b$ / %	$\sigma_b \pm s\sigma_b$ /MPa	E ± sE / MPa	Elastic modulus at 5 % elongation / MPa
100/0/0	505.5 ± 43.8	46.9 ± 4.1	120.8 ± 52.5	105.1 ± 41.1
100/0/1	726.3 ± 36.2	35.4 ± 3.0	109.1 ± 9.0	101.0 ± 9.0
100/0/2	677.0 ± 11.8	35.0 ± 2.7	99.3 ± 6.2	90.5 ± 6.2
100/0/3	654.5 ± 35.7	28.2 ± 2.5	69.3 ± 9.2	60.3 ± 6.2
90/10/0	56.7 ± 7.3	12.1 ± 0.7	239.0 ± 17.9	215.6 ± 14.1
90/10/1	46.0 ± 6.2	14.3 ± 1.8	228.5 ± 31.2	212.1 ± 16.4
90/10/2	28.7 ± 4.1	15.3 ± 2.4	216.0 ± 46.2	200.0 ± 17.7
90/10/3	40.3 ± 5.3	16.6 ± 3.0	179.5 ± 9.5	154.4 ± 2.2
80/20/0	19.4 ± 1.1	13.1 ± 1.0	352.2 ± 24.1	322.1 ± 12.2
80/20/1	17.5 ± 2.1	19.9 ± 1.0	420.3 ± 32.6	360.4 ± 11.9
80/20/2	16.5 ± 0.6	24.5 ± 1.5	428.6 ± 29.8	362.3 ± 29.8
80/20/3	19.4 ± 2.1	30.7 ± 0.8	435.9 ± 86.0	375.5 ± 52.9
60/40/0	15.8 ± 1.1	19.8 ± 0.2	523.3 ± 36.1	
60/40/1	9.9 ± 1.5	29.0 ± 3.6	273.0 ± 13.0	
60/40/2	10.1 ± 1.0	35.5 ± 3.6	582.2 ± 13.4	
60/40/3	9.6 ± 1.5	39.4 ± 0.1	553.2 ± 21.2	

ε_b, σ_b and E are respectively the elongation at break, stress at break, elastic modulus and Young's modulus; $s\varepsilon_b$, $s\sigma_b$ and sE are their standard deviations

3.2.3 Surface energy

Cross-linking and grafting should have an impact on the surface free energy. Figure 3.28 shows that the pure EVA matrix has a partially polar character, which is evident from the value of the polar component of the surface free energy. There is a decrease in the polar component and an increase in the non-polar component for DCP treated EVA. This must be the result of cross-linking which will give rise to a reduction in the number of polar vinyl acetate groups. The same trend is observed for EVA-sisal composites, prepared in the absence of DCP, where there is a decrease in the polar component and an increase in the non-polar

component with increasing sisal content. Sisal fibre consists of cellulose (strong polar character Figure 3.29), and therefore an increase in sisal content should increase the polar part of the surface free energy of the composites if there is no interaction between EVA and sisal fibre. As was mentioned before, grafting probably takes place through the OH groups in cellulose and the acetate groups in EVA, even in the absence of DCP, which will the number of polar groups in the samples. The decrease of the polar component and increase of the non-polar component become more evident with an increase in sisal fibre content. A slight increase in total surface energy with an increase in sisal fibre content was also observed (Figure 3.30). The surface energy data are summarized in Table 3.4.

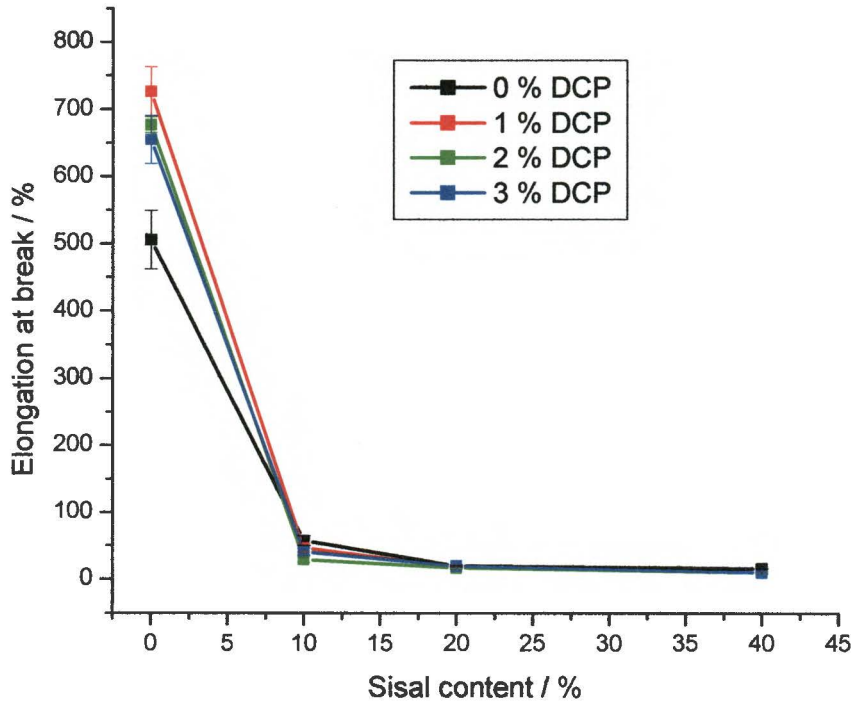

Figure 3.25 Effect of sisal content on the elongation at break of the composites

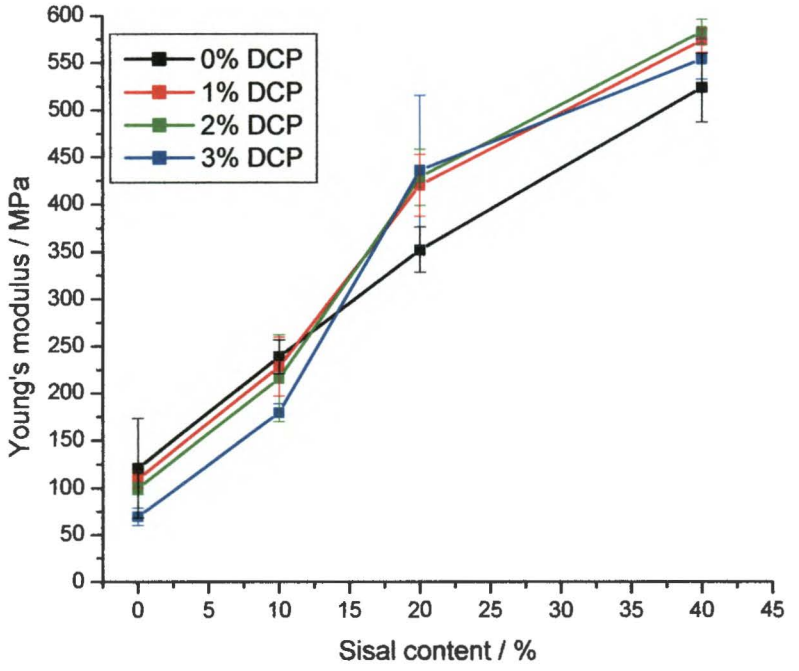

Figure 3.26 Effect of sisal content on Young's modulus of the composites

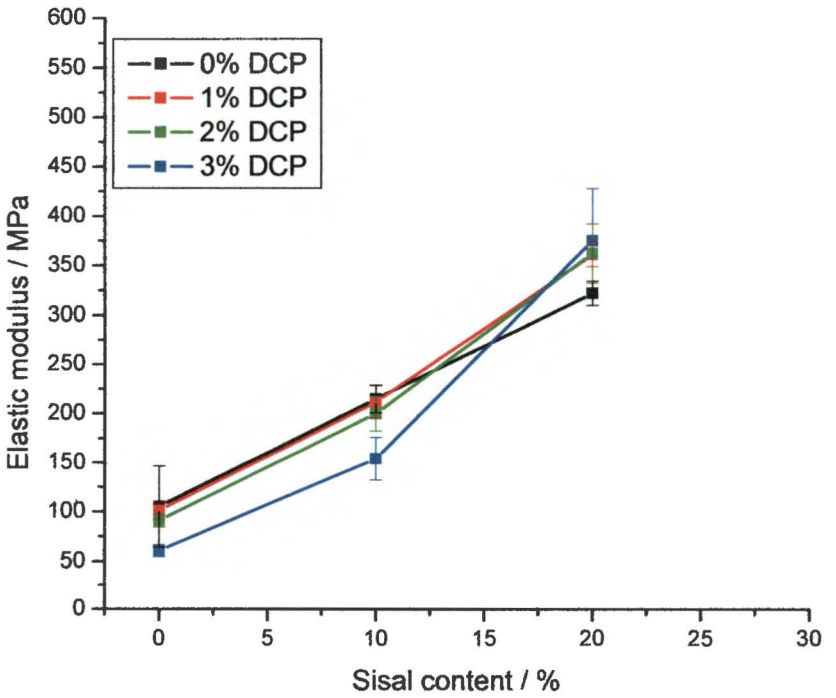

Figure 3.27 Effect of sisal content on Elastic modulus of the composites

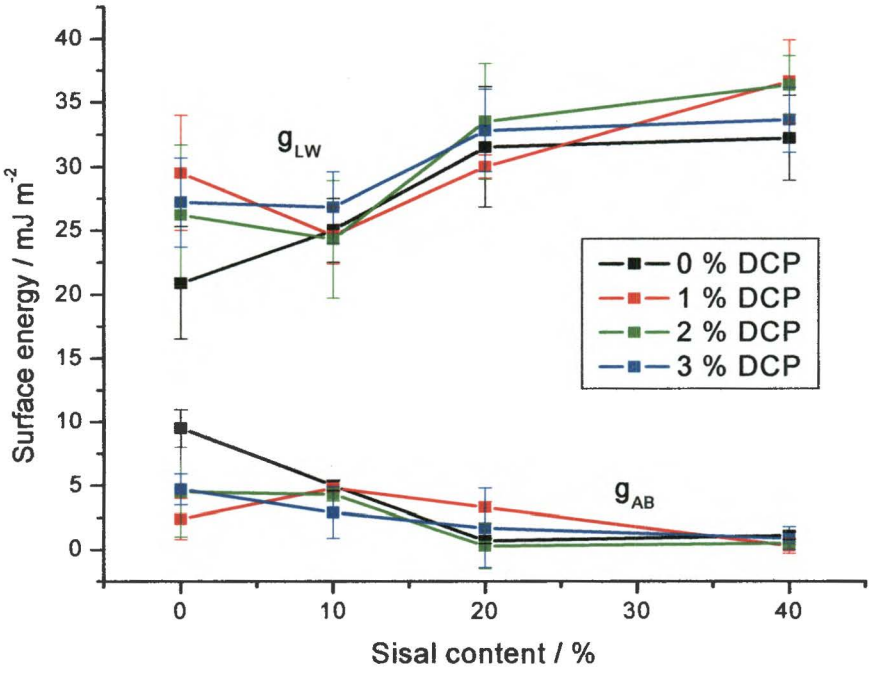

Figure 3.28 **Disperse (g_{LW}) and polar (g_{AB}) parts of the surface energy of EVA and its composites**

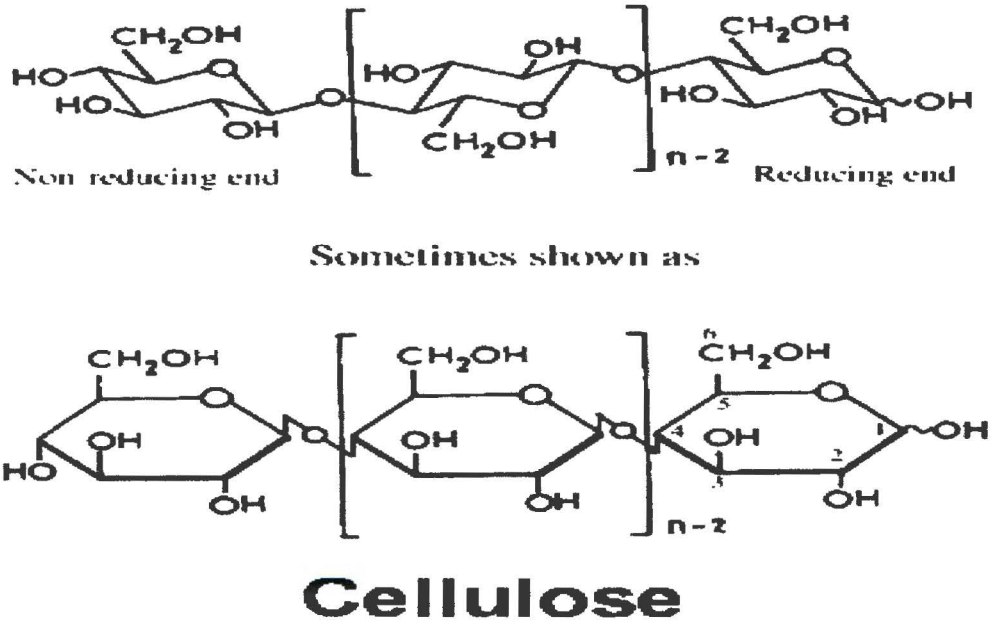

Figure 3.29 **Cellulose structure of sisal fibre**

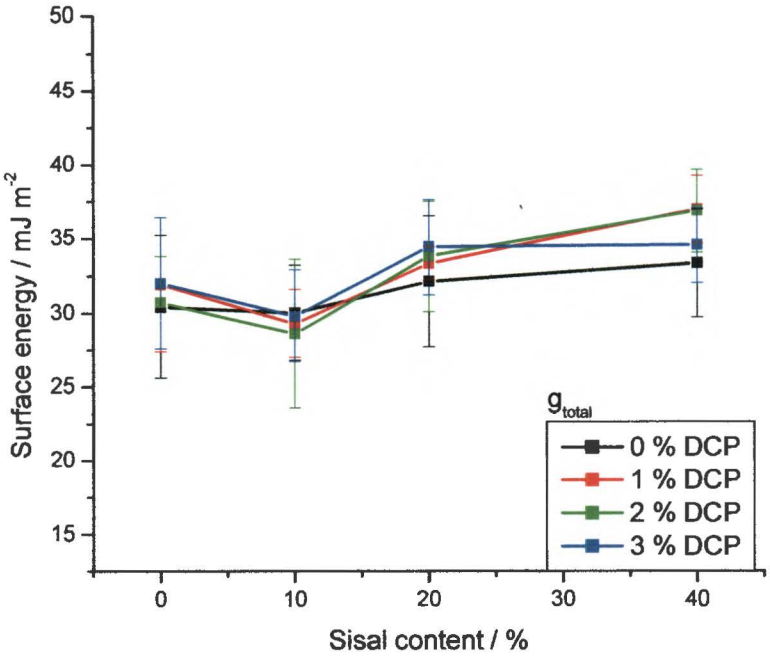

Figure 3.30 Total surface energy of EVA and its composites

Table 3.4 Surface energy data for untreated and DCP treated EVA-sisal composites

	100-0-00	**100-0-01**	**100-0-02**	**100-0-03**
g total	30.4	31.9	30.7	32.0
g LW	20.9	29.5	26.2	27.2
g AB	9.5	2.4	4.5	4.7
	90-10-00	**90-10-01**	**90-10-02**	**90-10-03**
g total	30.0	29.3	28.6	29.8
g LW	25.0	24.6	24.3	26.8
g AB	5.0	4.8	4.3	2.9
	80-20-00	**80-20-01**	**80-20-02**	**80-20-03**
g total	32.1	33.3	33.8	34.4
g LW	31.5	30.0	33.5	32.8
g AB	0.7	3.3	0.3	1.7
	60-40-00	**60-40-01**	**60-40-02**	**60-40-03**
g total	33.3	36.9	36.8	34.5
g LW	3.2	36.6	36.3	33.6
g AB	1.1	0.3	0.5	0.9

CHAPTER 4

CONCLUSIONS

It is well known that the physical properties of a polymeric material are strongly dependent on its morphology and structure. In composite materials, the interface between the matrix and filler also influences their properties.

In this work we presented and discussed the preparation and characterization of EVA-sisal fibre composites. All the results strongly point to grafting between EVA and sisal, even for samples prepared in the absence of DCP. Increasing the sisal content causes an increasing free volume of the EVA matrix, and hence the lamellar packing is influenced to such an extent that it gives rise to decreasing crystallinity and lamellar thickness. It does, however, seem as if cross-linking/grafting in the presence of DCP to a certain extent inhibits this influence.

Gel content results indicate increased cross-linking/grafting with increasing DCP and sisal contents. Grafting between EVA and sisal fibre is confirmed by the porosity and FTIR results. The SEM photomicrographs also support strong fibre-matrix adhesion in the EVA-sisal composites. Grafting, and to a lesser extent cross-linking of EVA, had an impact on the thermal and tensile properties of the composites, because cross-linking and grafting substantially influence the structure and morphology of the composites.

The incorporation of sisal in the EVA matrix increases the composites' stiffness. The influence of DCP on the stiffness, however, depends on the amount of sisal in the composite. For 0 and 10 % sisal, the tensile modulus decreases with increasing DCP content. For 20 and 30 % sisal, the tensile modulus increases with increasing DCP content, probably because of grafting between EVA and sisal. Elongation at break increases in the presence of DCP, but drastically decreases in the presence of sisal. For pure EVA, stress at break decreases with increasing DCP content, probably because of degradation. It also decreases when 10 % sisal is present in the EVA matrix, but increases for higher sisal contents. In the presence of sisal, increasing DCP content also increases stress at break, probably because of grafting between EVA and sisal.

Cross-linking and grafting also had an impact on the surface free energy of the samples. Generally the values of the polar component decreased with increasing sisal and DCP contents.

REFERENCES

1. Singh M and Garg M, *Construction and Building Materials,* **8**, 155-160 (1994)
2. Davis TJ and Claisse PA, *Construction and Building Materials,* **15**, 157-167 (2001)
3. Joseph K, Filho RDT, James B, Thomas S, de Carvalho, *Revista Brasileira de Engenharia Agricola e Ambiental*, **3**, 367-379 (1999)
4. Anil NN, *Research News, Materials Today*, **6**, 12-12 (2003)
5. Netravali AN and Chabba S, *Research News, Materials Today*, **6**, 22-29 (2003)
6. Glouston PL and Lam F, *Composites Science and Technology*, **62**, 1381-1395 (2002)
7. Lahellec N, Mazerolle F and Michel JC, *Journal of the Mechanics and Physics of Solids*, **52**, 27-49 (2004)
8. Humphreys FJ, Miller WS and Djazeb MR, *Materials Science and Technology*, **6**, 1156-1157 (1990)
9. Poudens A, Bacroix B and Bretheau T, *Material Science and Engineering A,* **196**, 1-2 (1995)
10. Poudens A and Bacroix B, *Scripta Materialia*, **34**, 847-855 (1996)
11. Chan HM and Humphreys FJ, *Metal Science*, **18**, 527-529 (1984)
12. Mizuuchi K, Inuoe K, Hanada K, Sugioka M, Itami M, Fukusumi M and Kawahara M, *Material Science and Engineering A*, **367**, 343-349 (2004)
13. Ho KF, Gupta M and Srivatsan TS, *Material Science and Engineering A*, **369**, 302-308 (2004)
14. Sinclair R, Press M, Marie E, Buffiere J–Y, Bowen P and Withers PS, *Acta Materialia*, **52**, 1423-1438 (2004)
15. Huang ZJ, Yang B, Cui H and Zhang JS, *Material Science and Engineering A*, **351**, 15-22 (2003)
16. Afaghani JED, Yamaguchi K, Nakamoto T and Yoshino K, *Wear*, **206**, 221-229 (1997)
17. Yin FS, Sun FX, Li JG, Guan HR and Hu ZQ, *Materials Letters*, **57**, 3377-3380 (2003)
18. Saraev D and Schmauder S, *International Journal of Plasticity*, **19**, 733-747 (2003)
19. Shimamoto A, Ohkawara H and Nogata F, *Engineering Fracture Mechanics*, **71**, 737-746 (2004)

20. Nguyen BN and Khaleel MA, *Composites Science and Technology*, **64**, 607-617 (2004)
21. Schjodt TJ and Pyrz R, *Composites Science and Technology*, **61**, 697-704 (2001)
22. Friedrich K, Reinicke R and Zhang Z, *Wear of Polymer Composites, Professional Engineering Publishing Ltd,* In Press (2002)
23. Zhang Z, Klein P and Friedrich K, *Composites Science and Technology*, **62**, 1001-1009 (2002)
24. Haddad MY and Feng J, *Composites Part B: Engineering*, **34**, 11-20 (2003)
25. Bledzki AK and Faruk O, *Composites Science and Technology*, **64**, 693-700 (2004)
26. Herrera-Franco PJ and Vlader-Gonzalez A, *Composites Part A: Applied Science and Manufacturing*, **35**, 339-345 (2004)
27. Govaert LE, d'Hooghe ELJCJ and Peijs AAJM, *Composites*, **22**, 113-119 (1991)
28. Peijs AAJM, Catsman P, Govaert LE, Lemstra BJ, *Composites*, **21**, 513-519 (1990)
29. Yao-hui L, Jun D, Si-rong Y and Wei W, *Wear*, **256**, 275-285 (2004)
30. Seymour RB, and Carraher Jr CE, *Polymer Chemistry, 3rd ed*, Marcel Dekker, New York (1992)
31. Suresh S, Mortensen A, Needleman A, *Fundamentals of Metal-Matrix Composites,* Elsevier (1993)
32. Brandrup J, Immergut EH and Gruke EA, *Polymer Handbook, 4th edn*, Willey, New York (1999)
33. Privalko EG, Pedosenko AV, Privalko VP, Walter R and Friedrich K, *Journal of Applied Polymer Science*, **73**, 1267-1271 (1999)
34. Kalaprasad G, Pradeep P, Mathew G, Pavithran C and Thomas S, *Composites Science and Technology,* **60**, 2967-2977 (2000)
35. Amash A and Zugenmaier P, *Journal of Applied Polymer Science,* **63**, 1143-1154 (1997)
36. Joseph K, Varghese S, Kalaprasad G, Thomas S, Prasannakumari L, Koshy P and Pavithran C, *European Polymer Journal,* **32**, 1243-1250 (1996)
37. Joseph K, Thomas S and Pavithran C, *Composites Science and Technology*, **53**, 99-110 (1995)
38. Maiti SN and Singh K, *Journal of Applied Polymer Science,* **32**, 4285-4292 (1998)
39. Li Y, Mai Y-W and Ye L, *Composites Science and Technology,* **60,** 2037-2055 (2000)
40. Bledzki AK and Gassan J, *Progress in Polymer Science,* **24**, 221-274 (1999)

41. Albano C, Gonzalez J, Ichazo M and Kaizer D, *Polymer Degradation and Stability*, **66**, 179-190 (1999)
42. Berlin AA, Volfson SA, Enikolopian NS and Negmator SS, *Principles of Polymer Composites*, edited by Henrici-Olive G and Olive S, Springer-Verlag (1986)
43. Herrera-Franco PJ, Valadez-Gonzales A and Cervantes-UCA, *Polymer Composites*, **28**, 331-343 (1997)
44. Chand N, Satyanarayana KG and Rohartgi PK, *Indian Journal of Textile Research*, **11**, 86-89 (1986)
45. Yang GC, Zeng HM and Zhang WB, *Cellulose Science and Technology*, **13**, 15-19 (1995)
46. Khalil HPSA, Ismail H, Rozman HD and Ahmad MN, *European Polymer Journal*, **37**, 1037-1045 (2001)
47. Yang GC, Zeng HM, Li JJ, Jian NB and Zhang WB, *Cellulose Science and Technology*, **35**, 53-57 (1996)
48. Joseph K, Thomas S and Pavitrhan C, *Polymer*, **37**, 5139-5149 (1996)
49. Sreekala MS and Thomas S, *Composites Science and Technology*, **63**, 861-869 (2003)
50. Rowell RM, Simonson R, Hess S, Plackett DV, Crenshaw D and Dunninghan E, *Wood Fibre Science*, **26**, 11-21 (1994)
51. Hill CAS, Khalil HPSA and Hale MD, *Industrial Crops and Products*, **8**, 53-62 (1988)
52. Mwaikambo LY, Martuscelli E and Avella M, *Polymer Testing*, **19**, 905-918 (2000)
53. Plackett D, Andersen TL, Pedersen WB and Nielsen L, *Composites Science and Technology*, **63**, 1287-1296 (2003)
54. Wollerdorfer M and Bader H, *Industrial Crops and Products*, **8**, 105-112 (1998)
55. Okman K, Skrifvars M and Selin J-F, *Composites Science and Technology*, **63**, 1317-1324 (2003)
56. Nishino T, Hirao K, Kotera M, Nakamae K and Inagaki H, *Composites Science and Technology*, **63**, 1281-1286 (2003)
57. Keller A, *Composites Science and Technology*, **63**, 1307-1316 (2003)
58. Bhagawan SS, Tripathy DK and De SK, *Journal of Applied Polymer Science*, **33**, 1623-1639 (2003)
59. Varghese S, Kuriakose B and Thomas S, *Journal of Natural Rubber Research*, **5**, 55 (1992)
60. Varghese S, Kuriakose B and Thomas S, *Journal of Applied Polymer Science*, **53**, 1051-1060 (1994)

61. Geethamma VG, Reethamma J and Thomas S, *Journal of Applied Polymer Science*, **55**, 583-594 (1995)
62. Coran AY,Boustany K and Hamed P, *Rubber Chemistry and Technology*, **47**, 396-401 (1974)
63. Prasant KR and Thomas S, *Bulletin of Materials Science*, **18**, 1021-1029 (1995)
64. Prasant KR and Thomas S, *Polymer International*, **38**, 173-187 (1995)
65. Paramasivam T and Abdulkalam APJ, *Fibre Science and Technology*, **1**, 85-98 (1974)
66. Pavithran C, Mukherjee PS, Brahmakumar M and Damodaran AD, *Journal of Material Science Letters*, **6**, 882-884 (1987)
67. Pavithran C, Mukherjee PS, Brahmakumar M and Damodaran AD, *Journal of Material Science Letters*, **7**, 825-826 (1988)
68. Joseph K, Thomas S and Pavithran C, *European Polymer Journal*, **32**, 10 (1996)
69. Satyanarayana KG, Sukumaran K, Mukherjee PS, Pavithran C and Pillai SGK, *Cement and Concrete Composites*, **12**, 117-136 (1990)
70. Bisanda ETN and Ansell MP, *Composites Science and Technology*, **41**, 165-178 (1991)
71. Maldas D and Kokta BV, *Polymer Degradation and Stability*, **31**, 9-12 (1991)
72. Kokta BV, *Polymer News*, **13**, 331-339 (1988)
73. Lightsey GR, Garrahen JR and Sperling LH, *Characteristics of Sisal Fibre,* Plenum Press (1983)
74. Raj RG, Kokta BV, Grolean G and Daneault G, *Plastics and Rubber Processing and Applications*, **11**, 205-221 (1989)
75. Raj RG and Kokta BV, *Journal of Applied Polymer Science*, **38**, 1987-1996 (1989)
76. Joseph K, Thomas S and Pavithran C, *Journal of Applied Polymer Science*, **47**, 1731-1741 (1993)
77. Kalaprasad G, Joseph K and Thomas S, *Journal of Materials Science*, **32**, 4261-4269 (1997)
78. Paul A and Thomas S, *Journal of Applied Polymer Science*, **63**, 247-266 (1997)
79. Paul A, Joseph K and Thomas S, *Composites Science and Technology*, **57**, 67-79 (1997)
80. Selzer R, *Advanced Composites Letters*, **4**, 87-90 (1995)
81. LeThi TT, Ganthier H, Gauthier R, Chabert B, Guillet J, Louong BV and Nguyen VT, *Journal of Material Science - Pure and Applied Chemistry*, **33**, 1997-2004 (1996)

82. Mokoena MA, Djokovic V and Luyt AS, *Journal of Materials Science*, **39**, 1-10 (2004)

83. Ichazo MN, Albano C, Gonzalez J, Perera R and Candal MV, *Composite Structures*, **54**, 207-214 (2001)

84. GiurgincaM, Popa L and Zaharescu T, *Polymer Degradation and Stability*, **82**, 463-466 (2003)

85. Martins MA, Mathe CG and Tavares MIB, *Polymer Testing*, **15**, 91 (1996)

86. Stael GC and Tavares MIB, *Polymer Testing*, **16**, 193-198 (1997)

87. Monteiro EEC and Thaumaturgo C, *Composites Science and Technology*, **57**, 1159-1165 (1997)

88. Stael GC, Tavares MIB and d'Almeide JRM, *Polymer Testing*, **20**, 869-872 (2001)

89. Sapieha S, Allard P and Zang YH, *Journal of Applied Polymer Science,* **41**, 2039 (1990)

ACKNOWLEDGEMENTS

I would like to thank most heartily all who assisted me during the course of the research for, and preparation of this thesis. In particular:

- I gratefully acknowledge my supervisor, Prof AS Luyt, for accepting me as his student as well as for excellent guidance on Polymer Science in general and on my work in particular.
- Mmê Motsei for her moral support.
- Dr H Krump for assisting with the interpretation of the results and L Jurica (from Customs Laboratories, Slovakia) for helping us in the FTIR sample analysis.
- The work was supported financially by the NRF and CSIR.
- My close friends (Tsietsi S Makhatha, Makgadiete G Salemane and Malefu A Bonene-Molaba) for being there for me.
- I also would like to thank my sister (Masehlomeng) and brothers (David Pule and Khotso) for all the support they have shown me.
- Technology has contributed to this work in one way or another and its developers are therefore also thanked.

Finally, my utmost thanks to the Almighty God for the opportunity to undertake this study and for His grace, without which this study would not have been possible.